The characterization of atomic interactions

R. F. W. Bader and H. Essén

Citation: J. Chem. Phys. **80**, 1943 (1984); doi: 10.1063/1.446956
View online: http://dx.doi.org/10.1063/1.446956
View Table of Contents: http://jcp.aip.org/resource/1/JCPSA6/v80/i5
Published by the American Institute of Physics.

The characterization of atomic interactions

R. F. W. Bader and H. Essén[a)]
Department of Chemistry, McMaster University, Hamilton, Ontario, Canada L8S 4M1

(Received 13 May 1983; accepted 30 November 1983)

The theory of molecular structure determined by the gradient vector field of the charge density ρ identifies the set of atomic interactions present in a molecule. The interactions so defined are characterized in terms of the properties of the Laplacian of the charge density $\nabla^2\rho(\mathbf{r})$. A scalar field is concentrated in those regions of space where its Laplacian is negative and depleted in those where it is positive. An expression derived from the quantum mechanical stress tensor relates the sign of the Laplacian of ρ to the relative magnitudes of the local contributions of the potential and kinetic energy densities to their virial theorem averages. By obtaining a map of those regions where $\nabla^2\rho(\mathbf{r}) < 0$, the regions where electronic charge is concentrated, one obtains a map of the regions where the potential energy density makes its dominant contributions to the energy of a system. It is demonstrated that atomic interactions fall into two broad general classes, closed-shell and shared interactions, each characterized by a particular set of mechanical properties. Interactions resulting from the sharing of charge density between atoms, covalent and polar bonds, are caused by a contraction of the charge density towards the line of interaction linking the nuclei. The curvatures of ρ perpendicular to the interaction line are dominant, electronic charge is concentrated in the internuclear region, and $\nabla^2\rho < 0$. These interactions are characterized by the large negative value of the potential energy in the internuclear region. Interactions between closed-shell atoms as found in noble gas repulsive states, in ionic bonds, in hydrogen bonds, and in Van der Waals molecules are governed by the contraction of the charge density towards each of the interacting nuclei. Thus one finds the parallel curvature of ρ to be dominant in these interactions, electronic charge is depleted in the interatomic surface and $\nabla^2\rho > 0$. The mechanics are characterized by the relatively large value of the kinetic energy, particularly the component parallel to the interaction line. In the closed-shell interactions, the regions of dominant potential energy contributions are separately localized within the boundaries of each of the interacting atoms or molecules. In the shared interactions, a region of low potential energy is contiguous over the basins of both of the interacting atoms. The problem of further classifying a given interaction as belonging to a bound or unbound state of a system is also considered, first from the electrostatic point of view wherein the regions of charge concentration as determined by the Laplacian of ρ are related to the forces acting on the nuclei. This is followed by and linked to a discussion of the energetics of interactions in terms of the regions of dominant potential and kinetic energy contributions to the virial as again determined by the Laplacian of ρ. The properties of the Laplacian of the electronic charge thus yield a unified view of atomic interactions, one which incorporates the understandings afforded by both the Hellmann–Feynman and virial theorems.

I. INTRODUCTION

The investigation of the properties of the electronic charge density is facilitated through the study of its associated fields. The topological properties of the charge density $\rho(\mathbf{r})$ are brought to the fore by its associated gradient vector field.[1,2] The properties of this field provide a definition of the elements of molecular structure.[3] The gradient vector field of $\rho(\mathbf{r})$ is topologically well-behaved and ideally suited for the application of modern mathematical theories of structure and structural stability.[4] A principal result of these theories is the demonstration that a definition of structure is inseparable from the notion of structural stability. Thus their application to the gradient vector field of the charge density yields a theory of molecular structure, an integral part of which is a definition of structural stability and a delineation of the mechanisms of structural change.[5,6]

The theory of molecular structure identifies the set of interatomic interactions present in a molecule, thereby quantifying the view of a molecule as a set of interacting atoms. It is the purpose of the present paper to characterize the properties of the atomic interactions so defined through a study of the properties of a scalar field derived from the charge density, its Laplacian distribution $\nabla^2\rho(\mathbf{r})$. According to Morse and Feshbach[7] the Laplacian is an extremely important property of a scalar field. It provides a direct determination of the regions where the field is concentrated. Aside from this intrinsic value, of determining where electronic charge is depleted and concentrated, the study of the Laplacian of the charge density is of particular importance as it provides a link between the form of $\rho(\mathbf{r})$ and its mechanical properties. The mechanics of the charge density are determined by the quantum stress tensor,[8,9] a quantity first introduced into quantum mechanics by Pauli,[10] It is shown,

[a)] Present address: Institute of Theoretical Physics, University of Stockholm, 5-11346 Stockholm, Sweden.

 0021-9606/84/051943-18$02.10

as a consequence of the properties of this stress tensor, that the sign of the Laplacian of $\rho(\mathbf{r})$ determines the relative magnitudes of the local values of the potential and kinetic energy densities. By obtaining a map of those regions where $\nabla^2\rho(\mathbf{r}) < 0$, the regions where electronic charge is concentrated, one obtains a map of the regions where the potential energy density makes its dominant contributions to the lowering of the energy of a system. The three local curvatures of $\rho(\mathbf{r})$, whose signs and relative magnitudes determine the sign of the Laplacian, are the eigenvalues of the Hessian matrix of $\rho(\mathbf{r})$. These same eigenvalues, evaluated at points where the gradient vector field of $\rho(\mathbf{r})$ vanishes, critical points of $\rho(\mathbf{r})$, determine the rank (the number of nonzero eigenvalues) and the signature (the algebraic sum of the signs of the eigenvalues) of these critical points. Such a classification summarizes in a concise manner the principal topological properties of a scalar field[2,11] including the stability or instability of the structure which it defines.[4,12] Thus there is an intimate link between the topological properties of $\rho(\mathbf{r})$ and its Laplacian, and through the properties of the Laplacian one may begin to bridge the gap between the form of the charge distribution and the mechanics which govern it.

II. MECHANICS OF AN ATOM AND OF THE CHARGE DENSITY

By imposing as a variational constraint on the principle of stationary action the equivalent mechanical statement of the topological definition of an atom, one obtains a definition of the average properties of an atom in a molecule.[9] In particular, one obtains a variational derivation of the Heisenberg equation of motion for the average value of the property A of atom Ω,[13]

$$\frac{dA(\Omega)}{dt} = \tfrac{1}{2}\{(i/\hbar)\langle[\hat{H},\hat{A}]\rangle_\Omega + \text{c.c.}\} + \oint dS\,[(\partial S/\partial t)\rho_A - \mathbf{J}_A\cdot\mathbf{n} + \text{c.c.})]. \quad (1)$$

The many-particle Lagrangian density $L(\psi, \nabla\psi, \dot{\psi}, t)$ and its corresponding single-particle density $L(\mathbf{r})$ are

$$L(\mathbf{r}) = \int d\tau'\, L(\psi, \nabla\psi, \dot{\psi}, t) = \int d\tau'\{(i\hbar/2)(\psi^*\dot{\psi} - \dot{\psi}^*\psi) - (\hbar^2/2m)\sum_i \nabla_i\psi^*\cdot\nabla_i\psi - \hat{V}\psi^*\psi\}. \quad (2)$$

When ψ satisfies Schrödinger's time-dependent equation, Eq. (2) reduces to

$$L(\mathbf{r}) = -(\hbar^2/4m)\nabla^2\rho(\mathbf{r}), \quad (3)$$

where $\rho(\mathbf{r})$ is the charge density. The derivation of the equation of motion for $A(\Omega)$ from the principle of stationary action is unique to a region of real space Ω whose Lagrangian $L(\Omega)$

$$L(\Omega) = \int_\Omega d\mathbf{r}\, L(\mathbf{r}) = (-\hbar^2/4m)\oint dS(\Omega;\mathbf{r})\nabla\rho(\mathbf{r})\cdot\mathbf{n}(\mathbf{r}) \quad (4)$$

vanishes as a consequence of the vanishing of the flux in $\nabla\rho$ at every point on the surface $S(\Omega;\mathbf{r})$ bounding the region Ω

$$\nabla\rho(\mathbf{r})\cdot\mathbf{n}(\mathbf{r}) = 0 \quad \forall\mathbf{r}\epsilon S(\Omega;\mathbf{r}). \quad (5)$$

Equation (5) is equivalent to the topological definition of an atom as the union of an attractor and its basin.[3,5] This definition is stated in terms of the gradient vector field of the charge density wherein the nuclei behave as point attractors (see Fig. 1).

The basins of neighboring atoms are separated by interatomic surfaces and their nuclei are linked by lines—atomic interaction lines—along which the charge density is a maximum with respect to any neighboring line (see Fig. 1). The network of interaction lines defines a molecular graph and the structure of the system. In general, a given structure

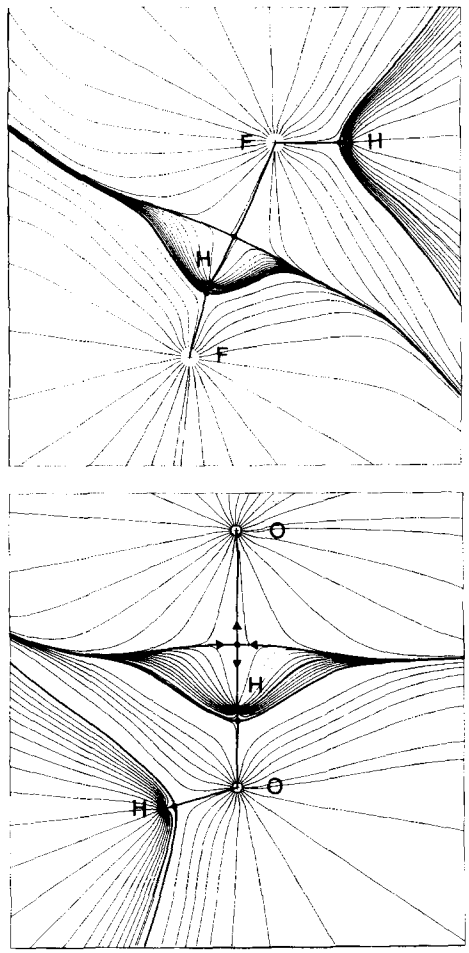

FIG. 1. Displays of the gradient vector fields of the charge density ρ for the hydrogen bonded dimers of HF and H_2O. The open cross in the lower diagram denotes the projected positions of the out-of-plane protons of the acceptor molecule. Each line represents a trajectory of $\nabla\rho$. A nucleus acts as an attractor of the $\nabla\rho$ field, i.e., all the trajectories in some open neighborhood of a nucleus, its associated basin, terminate at that nucleus. They are lines of steepest ascent through the charge density. An atom is the union of an attractor and its basin. Basins of neighboring atoms are separated by trajectories that *terminate* at a (3, −1) critical point (denoted by a black dot). In a symmetry plane a pair of such trajectories (shown as bold lines) terminate at each (3, −1) critical point. They denote the intersection of an interatomic surface with this plane. A pair of lines of steepest ascent (also shown as bold lines) *originate* at each (3, −1) critical point and terminate, one to each, at the neighboring nuclei. They define the atomic interaction lines—lines along which the charge density is a maximum with respect to any neighboring line. The directions of steepest ascent of the trajectories originating and terminating at a single (3, −1) critical point are indicated in the lower diagram. Since an interatomic surface is defined by the set of trajectories of $\nabla\rho$ terminating at a (3, −1) critical point, no trajectories cross such a surface Eq. (5), and the atomic Lagrangian vanishes Eq. (4).

persists over an open region of nuclear configuration space.[3,5]

Embodied in the definition of structure is the idea of relating the properties of a molecule to a set of pair-wise atomic interactions which dominate and characterize the mechanics underlying the structure. The interactions may be attractive or repulsive—the definition of structure in terms of the dominant interatomic interactions is essential to the understanding of either situation.

It is the purpose of this paper to demonstrate that atomic interactions as determined by this definition of molecular structure fall into two broad general classes, each characterized by a particular set of mechanical properties. It is shown that interactions between closed-shell atoms as found in noble gas repulsive states, in ionic bonds, in hydrogen bonds, and in van der Waal's molecules are governed by the contraction of the charge density towards each of the interacting nuclei. The mechanics of such interactions are dominated by the relatively large value of the kinetic energy, particularly the component parallel to the interaction line. Interactions resulting from the sharing of charge density between atoms, covalent and polar bonds, are governed by a contraction of the charge density towards the line of interaction linking the nuclei. The mechanics of these interactions are dominated by the large negative value of the potential energy in the internuclear region. In the closed-shell interactions, the regions of low potential energy are separately localized within the boundaries of each of the interacting atoms or molecules. In the shared interactions a region of low potential energy is contiguous over the basins of both of the interacting atoms. These are limiting classifications and there are interactions with properties which lie between those of the two limiting classes. The point to be emphasized is that there appear to be just two basic limiting mechanisms for atomic interactions—that the interaction giving rise to a van der Waal's molecule for example is more like, than it is different from that found in a hydrogen bonded system.[14] We begin with a review and further development of the necessary quantum mechanical relationships.

When the operator $\hat{A}$ in the Heisenberg equation of motion [Eq. (1)] is set equal to the momentum of an electron one obtains the atomic expression for the Ehrenfest force,[15] the force acting over the basin of atom Ω

$$\mathbf{F}(\Omega) = \int_\Omega d\mathbf{r} \int d\tau' \{\psi^*(-\nabla \hat{V})\psi\}$$

$$= m\int_\Omega d\mathbf{r}(\partial \mathbf{J}(\mathbf{r})/\partial t) - \oint dS(\Omega;\mathbf{r})\ddot{\sigma}(\mathbf{r})\cdot\mathbf{n}(\mathbf{r}). \quad (6)$$

In Eq. (6), $\hat{V}$ is the total potential energy operator, $\mathbf{J}$ the current density, and $\ddot{\sigma}$ the stress tensor, which may be expressed in terms of the first-order density matrix as

$$\ddot{\sigma}(\mathbf{r}) = (\hbar^2/4m)\{(\nabla\nabla + \nabla'\nabla')$$

$$-(\nabla\nabla' + \nabla'\nabla)\}\Gamma^{(1)}(\mathbf{r},\mathbf{r}')|_{\mathbf{r}=\mathbf{r}'}. \quad (7)$$

The current density is also expressible in terms of $\Gamma^{(1)}$ and hence Eq. (6) relates all of the one- and two-body forces acting on the electronic charge of an atom to gradients of $\Gamma^{(1)}$. In a stationary state, as is of interest here, the force acting on an atom is given by the integral of the force $\ddot{\sigma}\cdot d\mathbf{S}$ exerted on each element $d\mathbf{S}$ of its atomic surface by its neighboring atoms. An atomic surface $S(\Omega)$ is in general composed of a number of interatomic surfaces $S(\Omega,\Omega')$ and hence Eq. (6) may be expressed as

$$\mathbf{F}(\Omega) = -\int_\Omega d\mathbf{r}\, \nabla\cdot\ddot{\sigma}(\mathbf{r})$$

$$= -\sum_{\Omega'\neq\Omega}\oint dS(\Omega,\Omega';\mathbf{r})\ddot{\sigma}(\mathbf{r})\cdot\mathbf{n}(\mathbf{r}). \quad (8)$$

The sum in Eq. (8) runs over the atoms neighboring atom Ω—over each atom linked to Ω by an interaction line. Thus Eq. (8) provides the physical basis for the model in which a molecule is viewed as a set of interacting atoms. *It isolates, through the definition of structure, the set of atomic interactions which determines the force acting on each atom in a molecule for any configuration of the nuclei.*

When the operator $\hat{A}$ in Heisenberg's equation is set equal to $\hat{\mathbf{r}}\cdot\hat{\mathbf{p}}$ for an electron one obtains the virial theorem for an atom in a molecule. For a stationary state this theorem is

$$\mathscr{V}(\Omega) + 2T(\Omega) = -L(\Omega) = (\hbar^2/4m)\int_\Omega d\mathbf{r}\, \nabla^2\rho(\mathbf{r}), \quad (9)$$

where $\mathscr{V}(\Omega)$ is the virial of the forces acting over the basin and surface of the atom and $T(\Omega)$ is its average kinetic energy. Since the Lagrangian $L(\Omega)$ [Eq. (4)] vanishes for an atom in a molecule as it does for an isolated system, Eq. (9) reduces to the usual statement of the virial theorem,

$$0 = \mathscr{V}(\Omega) + 2T(\Omega). \quad (10)$$

A single theorem applies to an atom in a molecule, a linked grouping of atoms in a molecule or to the total isolated system. The kinetic energy $T(\Omega)$ is defined alternatively as

$$T(\Omega) = \int_\Omega K(\mathbf{r})d\mathbf{r}$$

$$= -(\hbar^2/2m)\int_\Omega d\mathbf{r}\{\nabla^2\Gamma^{(1)}(\mathbf{r},\mathbf{r}')|_{\mathbf{r}=\mathbf{r}'}\} \quad (11)$$

or

$$T(\Omega) = \int_\Omega G(\mathbf{r})d\mathbf{r}$$

$$= (\hbar^2/2m)\int_\Omega d\mathbf{r}\{\nabla\cdot\nabla'\Gamma^{(1)}(\mathbf{r},\mathbf{r}')|_{\mathbf{r}=\mathbf{r}'}\} \quad (12)$$

and the virial $\mathscr{V}(\Omega)$ as

$$\mathscr{V}(\Omega) = \int_\Omega d\mathbf{r}\{-\mathbf{r}\cdot\nabla\cdot\ddot{\sigma}(\mathbf{r}) + \nabla\cdot(\mathbf{r}\cdot\ddot{\sigma})\}$$

$$= \int_\Omega d\mathbf{r}\{-\mathbf{r}\cdot\nabla\cdot\ddot{\sigma}(\mathbf{r})\} + \oint dS(\mathbf{r})\mathbf{r}\cdot\ddot{\sigma}(\mathbf{r})\cdot\mathbf{n}(\mathbf{r}). \quad (13)$$

The two terms in Eq. (13) determine,respectively, the virials of the forces acting over the basin and the surface of the atom. Since $\mathscr{V}(\Omega)$ equals the virial of the forces exerted on the electrons in an atom Ω, or in the entire molecule (Ω = the total space of the system), it is by definition the average potential energy of the electrons in the atom Ω or in the entire molecule, respectively.

The Lagrangian of the Schrödinger field used to define the Lagrangian density in Eq. (2), may be used to define an energy-momentum tensor for the field. The spatial compo-

nents satisfy a set of divergence equations which, when integrated over the coordinates of all electrons but one, yield a differential expression of the Ehrenfest force law. The force acting on an element of electronic charge located at $\mathbf{r}$ is[8,16]

$$N\int d\tau'\,\psi^*(-\nabla\hat{V})\psi = \mathbf{F}(\mathbf{r},t) = m\partial\mathbf{J}(\mathbf{r})/\partial t - \nabla\cdot\ddot{\sigma}(\mathbf{r}). \tag{14a}$$

Integration of Eq. (14a) over an atomic basin yields directly the integrated force law Eq. (6). The force density $\mathbf{F}(\mathbf{r},t)$ is seen to be the total force exerted on the electron at position $\mathbf{r}_i$

$$-\nabla_i\hat{V} = \sum_\alpha Z_\alpha \nabla_i(|\mathbf{r}-\mathbf{X}_\alpha|)^{-1} - \sum_{j\neq i}\nabla_i(|\mathbf{r}_i-\mathbf{r}_j|)^{-1}$$

averaged over the motions of the remaining electrons

$$\mathbf{F}(\mathbf{r},t) = \left[\sum_\alpha Z_\alpha \nabla(|\mathbf{r}-\mathbf{X}_\alpha|)^{-1}\right]\rho(\mathbf{r}) - 2\int d\mathbf{r}'\,\nabla(|\mathbf{r}-\mathbf{r}'|)^{-1}\Gamma^{(2)}(\mathbf{r},\mathbf{r}'), \tag{14b}$$

where $\Gamma^{(2)}(\mathbf{r},\mathbf{r}')$ is the diagonal element of the two-density matrix normalized to $N(N-1)/2$. The force density $\mathbf{F}(\mathbf{r},t)$ may be interpreted as the total force exerted on the element of charge located at $\mathbf{r}$ and obeying an equation of motion in three-dimensional space Eq. (14a). For a stationary state, the force density is determined by the divergence of the stress tensor and is equal to the gradient of the so-called electrostatic potential $\Phi(\mathbf{r})$ multiplied by ρ

$$\Phi(\mathbf{r}) = -\sum_\alpha Z_\alpha(|\mathbf{r}-\mathbf{X}_\alpha|)^{-1} + \int d\mathbf{r}'\,\rho(\mathbf{r}')(|\mathbf{r}-\mathbf{r}'|)^{-1}, \tag{14c}$$

plus a contribution, which is nonconservative, arising from the correlated motions of the electrons.[17]

The virial of the force density for a stationary state yields the local expression of the virial theorem[8,9]

$$(\hbar^2/4m)\nabla^2\rho(\mathbf{r}) = -\mathbf{r}\cdot\nabla\cdot\ddot{\sigma}(\mathbf{r}) + \nabla\cdot(\mathbf{r}\cdot\ddot{\sigma}(\mathbf{r})) + 2G(\mathbf{r}) \tag{15}$$

an expression which upon integration, yields term for term the integrated expression for the virial theorem Eq. (9). In view of this correspondence, Eq. (15) will be rewritten as

$$-L(\mathbf{r}) = \mathscr{V}(\mathbf{r}) + 2G(\mathbf{r}), \tag{16}$$

where $L(\mathbf{r})$ is the Lagrangian density and $G(\mathbf{r})$ is the kinetic energy density of Eq. (12). Since the integration of $\mathscr{V}(\mathbf{r})$ yields $\mathscr{V}$, the average potential energy of the electrons, $\mathscr{V}(\mathbf{r})$ is the electronic potential energy density. In Eq. (16), the sum of the local contributions of the potential and kinetic energy densities to their virial theorem averages is related to a property of the charge density, its Laplacian $\nabla^2\rho(\mathbf{r})$. While their average values must satisfy the virial theorem [Eq. (10)] their local values in general do not and instead they satisfy Eq. (16). The kinetic energy density $G(\mathbf{r})$ is, by its definition, everywhere positive and $\mathscr{V}(\mathbf{r})$, which equals Tr $\ddot{\sigma}(\mathbf{r})$, is observed to be everywhere negative.[18] Thus the sign of the Laplacian of $\rho(\mathbf{r})$ determines which of the two contributions to the virial theorem, and hence to the total energy of the system, is dominant in a particular region of space. In addition, it is a property of the Laplacian of a scalar function that the function is concentrated in those regions where its Laplacian is negative.[7] Thus, Eq. (16) identifies the spatial regions of a molecule where the stabilizing contributions of the potential energy are dominant and simultaneously identifies these regions as those in which the electronic charge is locally concentrated.

The determination of the regions wherein a scalar field is concentrated throughout three-dimensional space is a nontrivial problem. The answer is provided by the properties of the Laplacian of the distribution as given in terms of its three competing curvatures at each point in space. The determination thus obtained is an absolute one made without recourse to a reference state. The properties of the Laplacian of the charge density are the subject of the following section.

III. PROPERTIES OF THE LAPLACIAN OF THE CHARGE DENSITY

In one dimension the curvature of $\rho(\mathbf{r})$ is a measure of the difference between its average value at points neighboring $\mathbf{r}$ and its value at $\mathbf{r}$.[7] The three-dimensional analogue is the Laplacian of ρ. A negative value for the Laplacian at some point means that electronic charge tends to concentrate at that point. As well as making quantitative in an absolute sense the notion of regions wherein charge is concentrated and depleted in terms of the curvatures of ρ, the Laplacian of the charge density plays an important theoretical role in the study of the charge density. As noted in the introduction, it determines the single-particle Lagrangian density of a quantum mechanical system.[8,16] While the integral over all space of the Laplacian of any well-behaved function vanishes, the vanishing of the corresponding integral of ρ has an important physical implication—that the action integral as well as the Lagrangian vanish for an isolated quantum system. This same property of ρ is observed for certain subsystems (atoms) of an isolated system and it is because of this common property that a single principle of stationary action applies to both the total molecule and to the atoms within it.[9] Finally, the Laplacian of ρ determines through the relative magnitudes of its three curvatures, the local imbalance in the contributions of the kinetic and potential energies to the virial of a system Eq. (16). It is this property of relating regions of concentration and depletion of charge to corresponding regions of dominant potential energy decrease and kinetic energy increase,respectively, that forms the basis for the classification of atomic interactions introduced in this work.

A. Laplacian distribution of atoms

While local maxima in a charge distribution occur only at the positions of nuclei, this observation does not imply that the contraction of ρ towards a nucleus is the dominant one at all distances from a nucleus, even in an isolated atom. Indeed this cannot be so for the atomic integral of $\nabla^2\rho(\mathbf{r})$ must vanish. Thus in addition to regions where the contraction of ρ along radial lines towards the nucleus is dominant and $\nabla^2\rho > 0$, there must exist a region or regions where the magnitudes of the curvatures of ρ perpendicular to these radial lines are dominant yielding negative values for the Laplacian of ρ. Thus $\nabla^2\rho(\mathbf{r})$ exhibits spherical nodes in an atom and their number is related to its shell structure. There are pairs of regions, one negative and one positive for each principal quantum shell with the innermost region where ρ is

a local maximum being negative. The first spherical node in a one-electron atom occurs at $r = 1/Z$ (Z = nuclear charge) and this is very nearly true for many-electron atoms as well, becoming increasingly exact as Z increases. The second node for the elements Li→Ne is found at a value of r a few tenths of an atomic unit greater than the radius of the core.[19] Thus one may associate paris of regions, one negative, one positive, with each principal quantum shell. The shell structure in $\nabla^2\rho(\mathbf{r})$ for an atom is illustrated in Fig. 2.

Since the only surface of zero flux in $\nabla\rho$ for an isolated atom occurs at infinity, the integral of $\nabla^2\rho$ over a pair of adjacent regions does not vanish except in the case of one- and two-electron atoms in their ground states which exhibit just one node. However, for the ground states of one-electron atoms one finds that the integral of $\nabla^2\rho(\mathbf{r})$ over the region where it is of one sign is proportional to the total energy $E(Z)$ of the atom

$$\frac{1}{4}\int_{\nabla^2\rho<0}\nabla^2\rho(\mathbf{r})d\tau = -\frac{1}{4}\int_{\nabla^2\rho>0}\nabla^2\rho(\mathbf{r})d\tau$$

$$= (4e^{-2})E(Z). \tag{17}$$

For such states, the greater the disparity in the average values of the potential and kinetic energies in regions where one quantity dominates the other, the lower is the total energy of the system.[20]

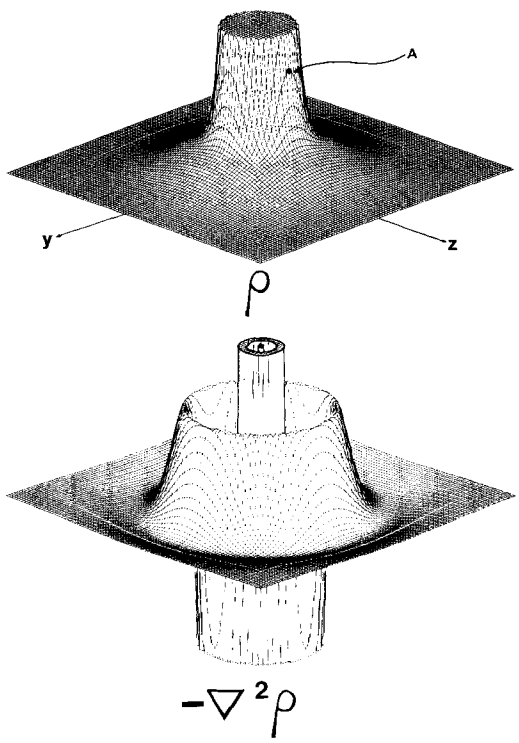

FIG. 2. The charge density and $-\nabla^2\rho$ are plotted on the third axis for a plane containing the nucleus of an argon atom. A maximum in $-\nabla^2\rho$ is a maximum in the concentration of electronic charge. At the point A, the curvature of ρ along z, the curvature along a radial line, is positive, while its curvature along the y-axis, a perpendicular curvature, is negative, as it also is along the x axis. If the sum of the magnitudes of the two perpendicular curvatures exceeds the value of the parallel curvature, $\nabla^2\rho<0$, and $-\nabla^2\rho$ indicates that electronic charge is concentrated at that point. In addition to the maximum at the nucleus there are two shells of charge concentration and three shells of charge depletion corresponding to the three quantum shells in this atom.

Thus, in an isolated atom there is a competition in the magnitudes of the positive curvature of ρ parallel to and of the negative curvatures perpendicular to a radial line along which ρ attains its maximum value at the position of the nucleus.[21] The result is a series of layered volumes in which the dominant contractions in ρ alternate between those parallel to and those perpendicular to the radial lines terminating at the nucleus.[22] The relative magnitudes of the contributions of the kinetic and potential energies to the virial from each region exhibit a corresponding alternation, the largest single contribution occurring from the excess of the potential energy over the kinetic energy in the region containing the nucleus where $\nabla^2\rho<0$.

B. Properties of the quantum force

An atom is a central field system and hence the force $\mathbf{F}(\mathbf{r})$ exerted on an element of charge is radially directed. This is the result anticipated on the basis of Eq. (14b) which relates $\mathbf{F}(\mathbf{r})$ to the gradients of electrostatic potential energy operators. To understand how contractions in ρ, particularly those perpendicular to a radial line, are related to and contribute to this force, to its virial and to the energy of an atom, it is necessary to consider the quantum expression for $\mathbf{F}(\mathbf{r})$,

$$\mathbf{F}(\mathbf{r}) = -\nabla\cdot\ddot{\sigma}(\mathbf{r}).$$

The stress tensor Eq. (7), can be written as

$$\ddot{\sigma}(\mathbf{r}) = -(\hbar^2/m)\{\nabla\nabla'\Gamma^{(1)}(\mathbf{r},\mathbf{r}')|_{\mathbf{r}=\mathbf{r}'}\} + (\hbar^2/4m)\nabla\nabla\rho(\mathbf{r}), \tag{18}$$

where $\nabla\nabla\rho(\mathbf{r})$ is the Hessian matrix of $\rho(\mathbf{r})$. The trace of this expression for $\ddot{\sigma}(\mathbf{r})$

$$\mathrm{Tr}\{\ddot{\sigma}(\mathbf{r})\} = -2G(\mathbf{r}) + (\hbar^2/4m)\nabla^2\rho(\mathbf{r})$$

is simply related to the kinetic energy density $G(\mathbf{r})$ and the Laplacian of $\rho(\mathbf{r})$. The stress tensor is thus determined by gradients of the state function and curvatures of $\rho(\mathbf{r})$. A stress tensor has the dimensions of an energy density or equivalently, of a force per unit area. The relation between the properties of $\ddot{\sigma}$ and its role in determining the force $-\nabla\cdot\ddot{\sigma}$ is obtained by writing $\ddot{\sigma}$ as

$$\ddot{\sigma}(\mathbf{r}) = \boldsymbol{\sigma}_x(\mathbf{r})\mathbf{i} + \boldsymbol{\sigma}_y(\mathbf{r})\mathbf{j} + \boldsymbol{\sigma}_z(\mathbf{r})\mathbf{k}, \tag{19}$$

where $-\boldsymbol{\sigma}_x dydz$ is the force exerted across the surface element $dy\,dz$, with corresponding expressions for $\boldsymbol{\sigma}_y$ and $\boldsymbol{\sigma}_z$. In general each of these forces has components both in and perpendicular to the surface element across which it acts. The *net* force acting on the infinitesimal volume element $dxdydz$ arising from the difference in $\boldsymbol{\sigma}_x$ from one face $dydz$ to the opposite face of the element is

$$dx(-\partial\boldsymbol{\sigma}_x/\partial x)dy\,dz$$

and the net force contributed by forces acting on all faces of the element is thus $-\nabla\cdot\ddot{\sigma}dx\,dy\,dz$, i.e.,

$$\nabla\cdot\ddot{\sigma} = \partial\boldsymbol{\sigma}_x/\partial x + \partial\boldsymbol{\sigma}_y/\partial y + \partial\boldsymbol{\sigma}_z/\partial z. \tag{20}$$

The important feature of this result is that the net force acting on an element of charge in one direction may have its origin in any or all of the forces acting across the faces of the element.

Consider a one-electron system for which the force is conservative and expressible in terms of a gradient of a potential Φ Eqs. (14b) and (14c). For the hydrogen atom $\Phi = -1/r$ and

$$\mathbf{F}(\mathbf{r}) = -\mathbf{a}_r\rho(\mathbf{r})/r^2,$$

where $\mathbf{a}_r = (\mathbf{r}/r)$, i.e., $\mathbf{F}(\mathbf{r})$ is radially directed. The quantum expression of this electrostatic force $-\nabla\cdot\overleftrightarrow{\sigma}$, or if one prefers, the quantum force which acts as the counterpose of the electrostatic force on $\rho(\mathbf{r})$ at each point in space Eq. (14a) with $\mathbf{J} = 0$, is expressed in terms of the gradients and curvatures of $\rho(\mathbf{r})$. The stress tensor for the H atom in atomic units is

$$\overleftrightarrow{\sigma}(\mathbf{r}) = (1/4)\{\nabla\nabla\rho - \nabla\rho\nabla\rho/\rho\} = (\rho/r)\{\mathbf{a}_r\mathbf{a}_r - \overleftrightarrow{1}\}, \quad (21)$$

where $\overleftrightarrow{1}$ is the unit dyadic. The interesting feature of Eq. (21) is that $\overleftrightarrow{\sigma}$ has no radially directed component $\mathbf{a}_r\cdot\overleftrightarrow{\sigma}(\mathbf{r}) = \mathbf{0}$. Thus if one considers a point $\mathbf{r}$ located on the z axis ($\mathbf{a}_r = \mathbf{k}$) the force exerted across the surface element $dx\,dy$ is zero and only the forces exerted across the faces parallel to z contribute to the net force on the element of charge at $\mathbf{r}$. Thus

$$\overleftrightarrow{\sigma}(0, 0, z) = \boldsymbol{\sigma}_x\mathbf{i} + \boldsymbol{\sigma}_y\mathbf{j}$$

and

$$-\nabla\cdot\overleftrightarrow{\sigma}(0, 0, z) = -(\partial\boldsymbol{\sigma}_x/\partial x) - (\partial\boldsymbol{\sigma}_y/\partial y)$$
$$= -\mathbf{k}\rho(0, 0, z)/z^2. \quad (22)$$

Even though the electrostatic force is radially directed and expressible in terms of the gradient of a potential, the equivalent quantum expression is entirely determined by stresses in the charge density acting across faces *parallel* to the direction of the net force.[23]

The virial of the force in Eq. (22) yields the potential energy density of the hydrogen atom, which along the z axis is simply $-\rho/z$ and $2G(\mathbf{r})$ is equal to $\rho(\mathbf{r})$. Equation (16) which relates the Laplacian to the kinetic and potential contributions to the virial becomes

$$(1/4)\nabla^2\rho(0, 0, z) = \rho - z(\partial\boldsymbol{\sigma}_x/\partial x)\cdot\mathbf{k} - z(\partial\boldsymbol{\sigma}_y/\partial y)\cdot\mathbf{k}. \quad (23)$$

The Laplacian of ρ is negative when the curvatures of ρ perpendicular to a radial line are dominant. From Eq. (23) this is the same region of space wherein the virials of the forces created by stresses in ρ across faces parallel to a radial line make the dominant contributions to the virial.

C. Laplacian distribution of molecules

The same competition between one positive and two negative curvatures of ρ in determining the sign of the Laplacian of ρ occurs when two atoms interact. Such an interaction results in the formation of an interjacent $(3, -1)$ critical point—one with two negative curvatures and one positive curvature (see Fig. 1). The eigenvectors associated with the two negative eigenvalues of the Hessian of ρ at the critical point (the two negative curvatures of ρ at $\mathbf{r}_c$) define a set of trajectories of $\nabla\rho(\mathbf{r})$ all of which terminate at the critical point. (The critical point behaves as a point attractor in two dimensions.) This set of trajectories defines the interatomic surface and clearly ρ is a local maximum in the interatomic surface at the position of the critical point—the point where the magnitudes of the negative curvatures are a maximum. The eigenvector associated with the single positive eigenval-

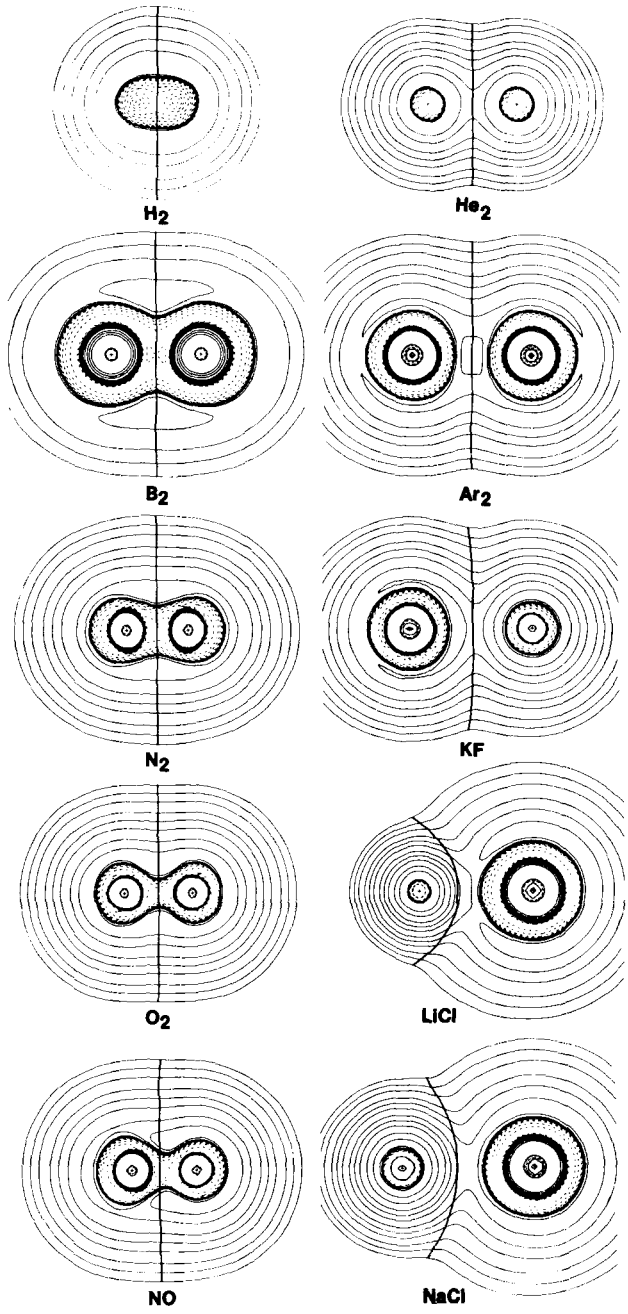

FIG. 3. Contour maps of the Laplacian of the charge density for molecules with shared and closed-shell interactions. Positive values of $\nabla^2\rho$ are denoted by solid contours, negative values by dashed contours. The Laplacian is also negative within the region bounded by the innermost solid contour enclosing the nucleus for all atoms beyond He in this and the remaining figures. The values of the contours in these and succeeding figures are not as important as the extent and relative positioning of the regions where $\nabla^2\rho$ is either positive or negative. Some contours overlap one another when $\nabla^2\rho$ undergoes a change in sign. The contour values in a.u. are ± 0.002, ± 0.004, ± 0.008 increasing in powers of 10 to ± 8.0. The outermost contour in each plot is $+0.002$ a.u. The intersection of each interatomic surface with the plane of the figure is also shown. The values of $\nabla^2\rho$ at the $(3, -1)$ critical points, the point where the interatomic surface intersects the atomic interaction line (which in these molecules is coincident with the internuclear axis) are recorded in Table I. In a shared interaction the region of charge increase is contiguous over the basins of both atoms and is a result of the contractions in ρ perpendicular to the interaction line. In a closed-shell interaction the regions of charge concentration are separately localized within each atom and the interaction is dominated by the contractions in ρ towards each of the nuclei.

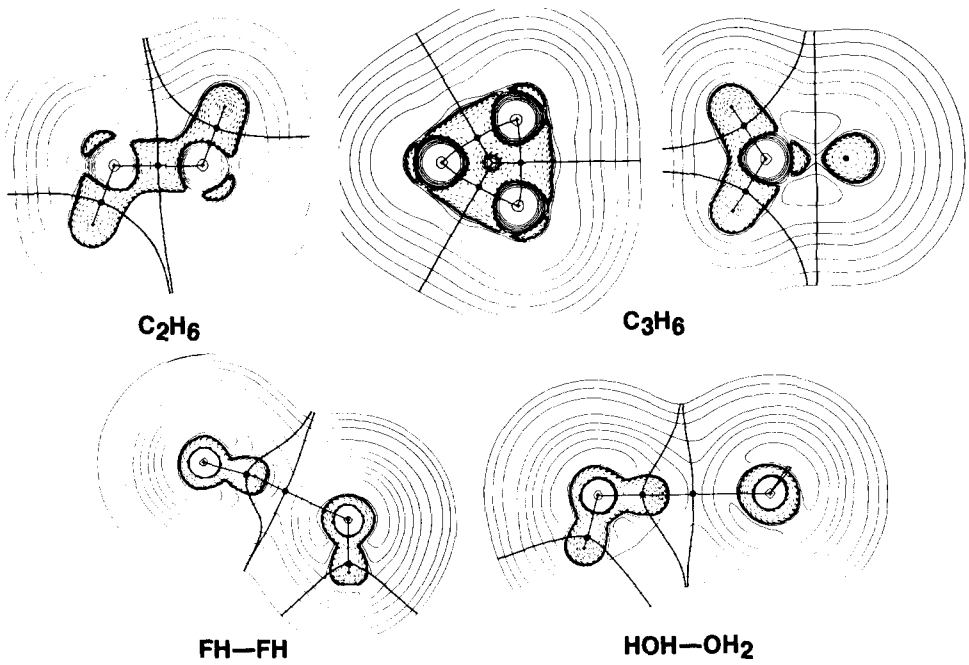

FIG. 4. Contour maps of the Laplacian of ρ for ethane, cyclopropane and the hydrogen bonded dimers of HF and H_2O. The (3, −1) critical points are indicated by black dots and interatomic surfaces are also indicated. The plane for C_2H_6 contains the nuclear framework H–C–C–H. The first diagram for C_3H_6 is for the plane containing three C nuclei. It is followed by a plane perpendicular to this containing a single C nucleus. The dot shown on the right-hand side of this diagram denotes the (3, −1) critical point defining the interaction line linking the two out-of-plane C nuclei. The bold line on the right-hand oxygen nucleus in $(H_2O)_2$ denotes the position of an out-of-plane H nucleus. The Laplacian is positive in the neighborhood of each hydrogen bond (3, −1) critical point—a closed-shell interaction. The associated interatomic surface defines the boundary of each monomer fragment. Note that the regions of charge concentration on the F and O nuclei of the proton acceptor fragments are polarized towards the hydrogen bonded proton.

ue of the Hessian at $\mathbf{r}_c$, the positive curvature, defines a unique pair of trajectories of $\nabla\rho$ each of which originates at $\mathbf{r}_c$ and terminates at one of the neighboring nuclei. Clearly, ρ is a minimum at $\mathbf{r}_c$ along this line of maximum charge density linking the two nuclei—the atomic interaction line.

An interatomic surface may be thought of as the basin of a two-dimensional attractor situated at the position of the interatomic critical point. This attractor is formed as a result of the interaction of the basins of two three-dimensional attractors. The two negative curvatures of ρ at $\mathbf{r}_c$ measure the degree of contraction of ρ in the interatomic surface, perpendicular to the interaction line *towards* this pseudo attractor. The positive curvature measures the degree of contraction of ρ parallel to the interaction line *away* from this pseudo attractor, towards each of the neighboring nuclei. If the negative curvatures dominate, electronic charge is locally concentrated in the region of the critical point (in the internuclear region) and the potential energy in this region has relatively large negative values (its magnitude is in excess of twice the kinetic energy from the same region) and the interaction is dominated by the low potential energy resulting from the formation of the (3, −1) or interatomic critical point. If, on the other hand, the positive curvature is dominant, ρ is concentrated separately in each of the atomic basins, and the interaction is dominated by the relatively large positive contributions to the kinetic energy of the system. The properties of ρ at an interatomic critical point, particularly its Laplacian, thus serves to summarize the interaction which creates the critical point. Laplacian distributions for diatomic and polyatomic molecules are shown in Figures 3 and 4. They exemplify the limiting cases where the atomic interaction is dominated by a region of charge accumulation ($\nabla^2\rho(\mathbf{r}_c) < 0$) in covalent and polar molecules, or by a region of charge depletion ($\nabla^2\rho(\mathbf{r}_c) > 0$) in noble gas, ionic and hydrogen bonded molecules.

An observation regarding the properties of $\rho(\mathbf{r})$ is that at most points in space it exhibits one positive and two negative curvatures. This is a result of $\rho(\mathbf{r})$ exhibiting local maxima only at the positions of nuclei and of an interaction between atoms resulting in the formation of a (3, −1) critical point. Thus this behavior of $\rho(\mathbf{r})$ is expected to be essentially ubiquitous in the neighborhood of a nucleus and in interatomic regions. It will depart from this behavior in the neighborhood of a (3, +1) or (3, +3) critical point in a structure containing a bonded ring or a bonded cage of atoms, respectively.

IV. CLASSIFICATION OF ATOMIC INTERACTIONS

Tables I and II give the properties of $\rho(\mathbf{r})$ at interatomic critical points for diatomic and polyatomic molecules. These are small samplings, meant to illustrate the characteristic limiting features of the two types of interaction, taken from a very large body of accumulated data. We first discuss the value of the charge density $\rho(\mathbf{r}_c)$ and its Laplacian $\nabla^2\rho(\mathbf{r}_c)$ at the interatomic critical points. The curvatures of ρ at $\mathbf{r}_c$ are denoted by λ_i. The two negative curvatures, which determine the contraction of ρ towards $\mathbf{r}_c$ in the directions perpendicular to the interaction line, are labeled λ_1 and λ_2. (In a linear molecule, $\lambda_1 = \lambda_2$.) The positive curvature of ρ at $\mathbf{r}_c$, the curvature parallel to the interaction line, is labeled λ_3.

The value of the Laplacian of ρ at $\mathbf{r}_c$ is negative for interactions between atoms in molecules at their equilibrium geometries for systems in which the interaction is usually described as covalent or polar. Since negative charge is concentrated along the line of interaction and shared by both nuclei in these systems they shall be referred to as *shared interactions*. The distribution of charge for a shared interaction is dominated by the negative curvatures of ρ. *Hence electronic charge is concentrated in the internuclear region as a result of the perpendicular contractions of ρ towards the interaction line, or equivalently in these bound systems, towards the bond path.*[24] This concentration of charge is reflected in the relatively large values of $\rho(\mathbf{r}_c)$, the value of ρ at the interatomic critical point. In most of these examples the

TABLE I. Characterization of atomic interactions.[a]

Molecule and state	R	$\rho(\mathbf{r}_c)$	$\nabla^2\rho(\mathbf{r}_c)$	Eigenvalues of Hessian of $\rho(\mathbf{r}_c)$: $\lambda_1=\lambda_2$ perpendicular	λ_3 parallel	$\lvert\lambda_1\rvert/\lambda_3$	Kinetic energy contributions: $G(\mathbf{r}_c)_\perp$	$G(\mathbf{r}_c)_\parallel$	$G_\perp/G_\parallel$	$G(\mathbf{r}_c)/\rho(\mathbf{r}_c)$	Net charge on A in AB
Shared interactions											
H_2 ($^1\Sigma_g^+$)	1.400	0.2728	−1.3784	−0.9917	0.6049	1.64	...	...	...	0.062[a]	
B_2 ($^3\Sigma_g^-$)	3.005	0.1250	−0.1983	−0.0998	0.0014	71.3	0.0223	0.0048	4.65	0.396	
N_2 ($^1\Sigma_g^+$)	2.068	0.7219	−3.0500	−1.9337	0.8175	2.37	0.3042	0.0170	17.89	0.866	
NO ($^2\Pi$)	2.1747	0.5933	−2.0353	−1.6460	1.2568	1.31	0.2366	0.0463	5.11	0.88	+0.495
NO^- ($^3\Sigma^-$)	2.1747	0.5755	−2.0851	−1.5883	1.0914	1.91	0.2284	0.0534	4.22	0.89	−0.088
O_2 ($^3\Sigma_g^-$)	2.282	0.5513	−1.0127	−1.4730	1.9333	0.76	0.2053	0.0721	2.85	0.88	
Closed-shell interactions											
He_2 ($^1\Sigma_g^+$)	3.000	0.0367	0.2501	−0.0774	0.4049	0.19	0.000	0.0540	0.000	1.47	
Ne_2 ($^1\Sigma_g^+$)	3.000	0.1314	1.3544	−0.3436	2.0417	0.17	0.0141	0.3024	0.047	2.52	
Ar_2 ($^1\Sigma_g^+$)	4.000	0.0957	0.4455	−0.1388	0.7231	0.20	0.0064	0.1144	0.056	1.33	
LiCl($^1\Sigma^+$)	3.825	0.0462	0.2657	−0.0725	0.4106	0.18	0.0033	0.0577	0.057	1.39	+0.924
NaCl ($^1\Sigma^+$)	4.461	0.0358	0.2004	−0.0401	0.2806	0.14	0.0035	0.0396	0.099	1.30	+0.911
NaF ($^1\Sigma^+$)	3.629	0.0543	0.4655	−0.0897	0.6449	0.14	0.0081	0.0890	0.090	1.94	+0.943
KF ($^1\Sigma^+$)	4.1035	0.0554	0.3132	−0.0717	0.4566	0.16	0.0067	0.0647	0.104	1.41	+0.930
MgO ($^1\Sigma^+$)	3.3052	0.0903	0.6506	−0.1331	0.9169	0.15	0.0170	0.1351	0.126	1.87	+1.412

[a] All quantities in atomic units. Results are calculated from functions using a Slater basis of near Hartree–Fock quality. Their sources are, P. E. Cade and A. C. Wahl, At. Data Nucl. Data Tables **13**, 339 (1974); P. E. Cade and W. M. Huo, *ibid.* **15**, 1 (1975); A. D. McLean and M. Yoshimine, IBM J. Res. Dev. **12**, 206 (1967); T. L. Gilbert and A. C. Wahl, J. Chem. Phys. **47**, 3425 (1967).

[b] A single determinant function for H_2 yields $G(\mathbf{r}_c)=0$. The value of $G(\mathbf{r}_c)/\rho(\mathbf{r}_c)$ is calculated from a correlated wave function for H_2; G. Das and A. C. Wahl, J. Chem. Phys. **44**, 87 (1966).

ratio $|\lambda_1|/\lambda_3$ is greater than unity. In cases of tight binding as evidenced by large negative values of $\nabla^2\rho(\mathbf{r}_c)$ as in N_2 e.g., λ_3 as well as λ_1 and λ_2 are large in magnitude, but the ratio $|\lambda_1|/\lambda_3$ is still greater than unity. When the antibonding 2π orbital of AB molecules or the π_g orbital of homonuclear diatomics is occupied, λ_3 increases. Compare, e.g., λ_3 for NO, NO^-, and O_2 with that for N_2.

For shared interactions, as illustrated in Figs. 3 and 4, the region of space over which the Laplacian of ρ is negative and which contains the interatomic critical point is contiguous over the valence regions of both atoms. The interactions result in a sharing of valence density which leads to a single region of relatively low potential energy extending over both atomic basins.

Further examples of shared interactions are given in Table II for polyatomic systems. The value of $\rho(\mathbf{r}_c)$ for carbon–carbon bonds may be used to establish a bond order which in turn provides a reasonable electron count for such bonds.[25] In the absence of axial symmetry the two perpendicular curvatures of ρ at $\mathbf{r}_c$ are not in general degenerate. In CC bonds the orbital model of π bonds is reflected in the magnitude of one such curvature being less than the other

TABLE II. Characterization of atomic interactions.[a]

Molecule and interaction	R	$\rho(\mathbf{r}_c)$	$\nabla^2\rho(\mathbf{r}_c)$	λ_1	λ_2	λ_3	$\lvert\lambda_1\rvert/\lambda_3$	$G(\mathbf{r}_c)_\perp$[b]	$G(\mathbf{r}_c)_\parallel$	$G_\perp/G_\parallel$	$G(\mathbf{r}_c)/\rho(\mathbf{r}_c)$
Shared interactions											
CC bond in ethylene	2.489	0.3627	−1.1892	−0.8147	−0.5635	0.1890	4.31	0.0674	0.0040	16.85	0.383
CC bond in benzene	2.619	0.3268	−1.0134	−0.7070	−0.5746	0.2682	2.64	0.0460	0.0037	12.43	0.293
CC bond in ethane	2.886	0.2523	−0.6615	−0.4772	−0.4772	0.2929	1.63	0.0223	0.0048	4.65	0.196
CC bond in cyclopropane	2.830	0.2490	−0.5331	−0.4892	−0.3284	0.2846	1.72	0.0382	0.0073	5.23	0.336
CH bond in CH_4	2.048	0.2770	−0.9784	−0.7178	−0.7178	0.4571	1.57	0.0180	0.0030	6.00	0.141
OH bond in H_2O	1.782	0.3909	−2.4416	−2.0658	−2.0081	1.6323	1.27	0.0339	0.0141	2.40	0.210
OH bond in proton donor of $(H_2O)_2$	1.790	0.3825	−2.5346	−2.1187	−2.0645	1.6486	1.29	0.0310	0.0139	2.40	0.198
FH	1.691	0.4043	−3.8426	−2.8882	−2.8882	1.9338	1.49	0.0401	0.0185	2.17	0.244
FH bond in proton donor of $(HF)_2$	1.712	0.3846	−3.8643	−2.8202	−2.8202	1.7759	1.59	0.0357	0.0196	1.82	0.236
Closed-shell interactions											
Hydrogen bond in $(H_2O)_2$	3.853	0.0198	0.0623	−0.0247	−0.0240	0.1110	0.223	0.0061	0.0147	0.415	0.806
Hydrogen bond in $(HF)_2$	3.360	0.0262	0.1198	−0.0406	−0.0360	0.1994	0.204	0.0013	0.0243	0.053	1.027

[a] All quantities in atomic units. The data are calculated from single determinant Gaussian basis state functions at corresponding optimized geometries: a 6-31G* basis was used in the hydrocarbon calculations, a 6-31G** basis for the monomer and dimer calculations of H_2O and HF.

[b] This is the average value of the two perpendicular components.

indicating the preferred accumulation of charge in a particular plane containing the bond path. The ellipticity of a bond defined as $\epsilon = (\lambda_1/\lambda_2 - 1)$ where $|\lambda_1| > |\lambda_2|$, provides a measure of the deviation of the charge density along the bond path from radial symmetry.[25] The ellipticity provides a sensitive measure of the degree of "π character" of a bond and in more general terms, a measure of the extent to which electronic charge is preferentially accumulated in a particular plane. One notes that as $\rho(\mathbf{r}_c)$ decreases for *CC* bonds through the series ethylene to ethane, the value of $\nabla^2\rho(\mathbf{r}_c)$ becomes less negative. Correspondingly, for a long CC bond of order less than one, the depletion of charge in the interatomic surface results in a further increase in the parallel curvature λ_3 and $\nabla^2\rho(\mathbf{r}_c)$ approaches zero.[25]

The second limiting type of atomic interaction is that occurring between closed-shell systems as illustrated by the second sets of entries in Tables I and II. One anticipates that such interactions will be dominated by the requirements of the Pauli exclusion principle. Thus for *closed-shell interactions* $\rho(\mathbf{r}_c)$ is relatively low in value and the value of $\nabla^2\rho(\mathbf{r}_c)$ is positive. *The sign of the Laplacian is determined by the positive curvature of ρ along the interaction line as the exclusion principle leads to a relative depletion of charge in the interatomic surface. These interactions are dominated by the contraction of charge away from the interatomic surface towards each of the nuclei.* The Laplacian of ρ is positive over the entire region of interaction and the kinetic energy contribution to the virial from this region is greater than the contribution from the potential energy. The spatial displays of the Laplacian of ρ given in Fig. 3 are atomic-like. The regions where the Laplacian is negative are, aside from small polarization effects to be discussed later, identical in form to those of a free atom or ion. Thus the spatial regions where the potential energy dominates the kinetic energy are confined separately to each atom, reflecting the contraction of the charge towards each nucleus, away from the region of the interatomic surface. The ratio $|\lambda_1|/\lambda_3 < 1$ in all the examples of closed-shell interactions.

The almost complete interatomic transfer of one electronic charge indicated in Table I for the ionic systems is verified by the nodal structure of the corresponding Laplacian maps. The cations Li^+, Na^+, and K^+ all lack the outer nodes associated with the valence density distribution of the isolated atom. Thus Li in LiCl has but one negative region rather than two, Na in NaCl has two rather than three and K in KF has three rather than four.

Data for the hydrogen bonds in the dimers of HF and H_2O are given in Table II. A hydrogen bond results from the interaction of two closed-shell systems and the properties of ρ at the associated bond critical point reflect all of the characteristics associated with such interactions; a low value for $\rho(\mathbf{r}_c)$ and $\nabla^2\rho(\mathbf{r}_c) > 0$. Each HF or H_2O fragment is easily recognizable in the display of the Laplacian for the corresponding dimer. None of the characteristics associated with the sharing and accumulation of charge are evident in the neighborhood of a hydrogen bond critical point. The negative regions of the Laplacian are separately localized in each HF fragment in a pattern similar to that of an isolated HF molecule. The Laplacian map for the dimer of HF is topologically equivalent (i.e., continuously deformable) into that for Ne_2. Why certain closed-shell interactions are stable with respect to separated species while others are not, is intimately related to the extent of interatomic charge transfer and to the polarization of the atomic distributions. The distinctions between bonded and repulsive interactions is discussed in Sec. V.

Also included in Tables I and II are the values of the kinetic energy density at the interatomic critical point $G(\mathbf{r}_c)$ and its parallel and perpendicular components. It is clear from the definition of the density $G(\mathbf{r})$ [Eq. (12)] that it is expressible in terms of three contributions along axes determined by the eigenvectors of the Hessian of ρ at $\mathbf{r}_c$. The relative values of the parallel ($G_\parallel$) and one of the perpendicular ($G_\perp$) components of the kinetic energy density faithfully reflect the values of the corresponding curvatures of ρ at $\mathbf{r}_c$. For the shared interactions, $G_\perp(\mathbf{r}_c) > G_\parallel(\mathbf{r}_c)$, while just the reverse situation is found for the closed-shell interactions. In addition, as anticipated on the basis of Eq. (16), the kinetic energy per electronic charge, the ratio $G(\mathbf{r}_c)/\rho(\mathbf{r}_c)$, is less than unity for the shared interactions and greater than unity for the closed-shell interactions. Thus when the positive curvature of ρ is large and dominant as a result of the contraction of the charge towards the nuclei, the kinetic energy per electron is absolutely large and the value of its parallel component exceeds that of a perpendicular component. In the shared interactions, the accumulation of charge in the internuclear region leads to a softening of the gradients of ρ and of the corresponding curvature of ρ along the interaction line and the parallel component of $G(\mathbf{r})$ is correspondingly less than its perpendicular components. The dominance of these latter components again mirror the corresponding dominance of the perpendicular contractions of ρ towards the bond axis in shared interactions. Because of the concentration of charge and the concomittant negative values of the Laplacian of ρ over the same region, the potential energy is dominant, and the kinetic energy per electron is absolutely small.

The same observations regarding the behavior of the parallel and perpendicular components of the kinetic energy and their relation to the gradients and curvatures of ρ in molecular systems were first made by Bader and Preston[26] for the molecules H_2 and He_2. The kinetic energy density $G(\mathbf{r})$ and its components may be related directly to the gradients of the orbital densities ρ_i and their occupation numbers n_i,

$$G(\mathbf{r}) = (\hbar^2/8m)\sum_i n_i \nabla\rho_i \cdot \nabla\rho_i/\rho_i. \tag{24}$$

For a one-electron system, Eq. (24) relates $G(\mathbf{r})$ to the gradients of $\rho(\mathbf{r})$ itself. For H_2, where just one orbital ($1\sigma_g$) and for He_2, where just two orbitals ($1\sigma_g$ and $1\sigma_u$) make the major contributions to ρ, the above observations regarding the paralleling behavior of $G_\perp(\mathbf{r})$ and $G_\parallel(\mathbf{r})$ with that of the corresponding gradients and curvatures of ρ for the shared and closed-shell interactions are immediately made clear by Eq. (24).[26] However, the data in Tables I and II show that these are general observations, and that even in many-electron systems the local behavior of the kinetic energy density may be related to the gradients and curvatures of the total charge

density. This correlation is partially accounted for by theory through Eq. (16). When $\nabla^2\rho(\mathbf{r}) > 0$ and the Laplacian is dominated by the positive curvature of ρ (contraction of ρ towards a nucleus), the larger contribution to the Laplacian comes from the kinetic energy—and by observation, primarily from its parallel component. Correspondingly, when the Laplacian of ρ is negative and ρ is concentrated as a result of contractions perpendicular to the radial lines terminating at a nucleus, not only does the potential energy make the dominant contribution to the virial but one observes the perpendicular components of $G(\mathbf{r})$ to dominate its parallel component. Thus one concludes that the kinetic energy dominates the contributions to the virial and to the energy in regions of space where its parallel component is dominant. This occurs in regions where $\nabla^2\rho(\mathbf{r}) > 0$. Conversely in regions where the perpendicular components of $G(\mathbf{r})$ are largest, the potential energy makes the major contribution to the virial and to the energy of the system.

As noted by Bader and Preston,[26] the differing behavior of $G_{\parallel}(\mathbf{r})$ and $G_{\perp}(\mathbf{r})$ in H_2 is so extreme as to be reflected in their integrated average values.[27] Thus, the ratio of the average values of the parallel ($T_{\parallel}$) to the sum of the perpendicular ($T_{\perp}$) components of the kinetic energy for H_2 at its equilibrium separation was found to be 0.3569 as compared to the value of one-half for the separated atoms. As noted by these authors, this result is consistent with the original observation made by Coulson[28] in his study of the electronic momentum distribution for the H_2 molecule. He found that the mean component of the electronic momentum in the direction of the bond axis is decreased while the mean component perpendicular to the bond axis is increased. From the present study, this behavior should be general (but not as pronounced as for H_2) for shared interactions, as is verified by Compton scattering experiments. Epstein and Tanner[29] have incorporated Coulson's observation in a proposed bond directional principle for the interpretation of Compton scattering results. The present analysis however, shows that this cannot be a general principle but one which is restricted to bonds arising from shared interactions. For closed-shell interactions, just the opposite behavior will be obtained. Bader and Preston[26] noted that in He_2, which typifies such interactions, $G_{\parallel}(\mathbf{r}) > G_{\perp}(\mathbf{r})$ and found $T_{\parallel}/T_{\perp} > 0.5$. This dominance of the parallel over perpendicular components of T, both locally and overall, is anticipated on the basis of the Laplacian map for He_2 which is everywhere positive except for small spherical regions encompassing each nucleus (Fig. 3). These properties of the kinetic energy are also evident in the electron momentum distribution of He_2. Ramirez[30] finds that this distribution in He_2 is ellipsoidal with major axis parallel to the line of interaction, just the opposite of the situation found in H_2 where the major axis of the momentum distribution is perpendicular to the bond axis as found by Coulson.[28] Cade and Henneker,[31] in a comparative study of the electron momentum distributions of N_2 and LiF, note that in N_2 the momentum is greater $\perp$ to the molecular axis than it is $\parallel$ to this axis, while in LiF there is a near independence of the distribution with respect to the direction of this axis. Their contour plot of the momentum distribution for LiF does however, exhibit a small preponderance of the parallel over the perpendicular components as anticipated for a closed-shell interaction.

Weyrich[32] and Pattison and Weyrich[33] have used the autocorrelation function (the Fourier transform of the momentum space density) for the interpretation of experimental Compton profiles. This quantity is a function of the position space variables. Its properties are ideally suited for the determination of the consequences of the repulsions between the (diffuse) closed-shell anions on the charge distribution of an ionic crystal. The repulsions are treated as arising as a consequence of orthogonality constraints on the crystal orbitals. Interestingly enough, the autocorrelation function exhibits the same behavior for the hydrogen bonds in liquid water as it does for the anions in crystals and is similarly interpreted as being a consequence of the interaction of two closed-shell systems,[32] in agreement with the classification of hydrogen bonds given here.

A. Intermediate interactions

The examples so far considered illustrate that atomic interactions exhibit two limiting sets of behavior, one set being the opposite of the other in terms of the regions of charge concentration and depletion and the associated mechanical consequences as determined by the sign of the Laplacian of ρ. In these examples, the interatomic critical point is situated relatively far from a nodal surface in the Laplacian of ρ and the interaction is typified by the behavior of ρ at $\mathbf{r}_c$. In some molecules, however, the critical point is located close to a nodal surface in $\nabla^2\rho$ and the atomic basins neighboring the interatomic surface exhibit opposite behavior with respect to the sign of the Laplacian of ρ. The transition from closed-shell to shared interactions is illustrated in Fig. 5 for the second- and third-row diatomic hydrides, *AH*. The properties of $\rho(\mathbf{r})$ at the interatomic critical points for these molecules are given in Table III. The first member of each series LiH and NaH, exhibits the characteristics of a closed-shell interaction. The charge density of a hydrogen atom is easily polarized, particularly when it is negatively charged. This polarization is evident in the disposition of the negative region of $\nabla^2\rho$ relative to the position of the proton. The Laplacian distributions and the properties at $\mathbf{r}_c$ for the molecules CH to FH and SH to ClH are typical of shared interactions. In CH there is a close to zero transfer of charge and an equal sharing of the charge increase. In NH, OH, and HF there is an increasing polarization of the shared charge towards A. The transition to a shared interaction occurs earlier in the second-row than in the third-row elements as anticipated on chemical grounds and is understandable in terms of the greater core size of a third-row element compared to a corresponding second-row element.

The values of $\rho(\mathbf{r}_c)$ show a monotonic increase through both series, being a minimum at the closed-shell limit. In BeH to BH and MgH to SiH the valence charge density remaining on A is strongly polarized into the nonbonded region of the A atom (as a consequence of the net negative field exerted on it by the negatively charged hydrogen atom) where it forms a separate region of charge increase. For these molecules and for PH the ratios $|\lambda_1|/\lambda_3$, $G_{\perp}(\mathbf{r}_c)/G_{\parallel}(\mathbf{r}_c)$, and $G(\mathbf{r}_c)/\rho(\mathbf{r}_c)$ exhibit values intermediate between those char-

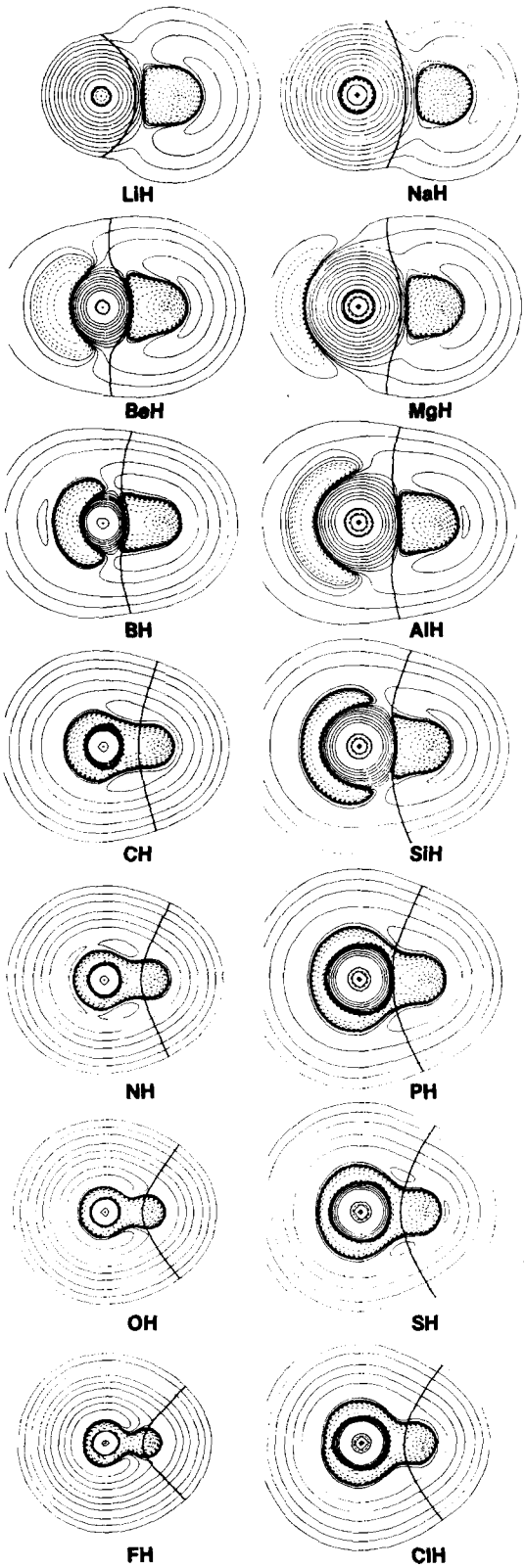

FIG. 5. Contour maps of the Laplacian of ρ for second- and third-row diatomic hydrides. These maps illustrate the transition from closed shell to shared atomic interactions. See Table III for values of $\nabla^2\rho$ at (3, −1) critical points.

acteristic of the two limiting types of interactions. The atomic interactions in these molecules have properties which bridge those of the ionic systems at the closed-shell limit and those of the covalent and polar systems of the shared interactions. In molecules such as BeH, BH, and SiH where the nodal surface in $\nabla^2\rho$ is nearly coincident with the interatomic surface, the atomic interactions correspond to a relatively hard core of density on the A atom which is dominated by contractions towards the A nucleus, interacting with a softer more polarizable region of charge concentration on the bonded side of the proton which is dominated by contractions of ρ towards the bond path.[34]

A carbon–oxygen bond is another atomic interaction wherein the nodal surface in $\nabla^2\rho$ is nearly coincident with the interatomic surface. This is illustrated by the Laplacian maps of ρ in Fig. 6 for carbon monoxide, formaldehyde and methanol. In all three molecules there is charge transfer ranging from 1.2 to 1.3 electronic charges from carbon to oxygen. In CO the remaining valence charge on C is very strongly polarized into its nonbonded region as is evident in its Laplacian map and in its total density distribution. There are large dipoles present in both atomic distributions particularly on C with directions counter to the direction of charge transfer. The atomic dipoles nullify the charge transfer moment and the resultant dipole moment is near zero. In formaldehyde the remaining valence density on carbon is employed in bonding the hydrogens in shared non polar interactions, typical of CH bonds, compare with CH in Fig. 5. [Note the small region of charge concentration on the nonbonded side of C (w.r.t. oxygen) in the plane perpendicular to the plane of the nuclei relative to the corresponding region in CO (Fig. 6).] Thus the carbon atom of formaldehyde does not possess a significant atomic dipole and this molecule exhibits a net dipole moment as a result of the charge transfer from C to O. One notes by comparing these three C–O interactions and the C–H and O–H interactions with those given in previous figures, that each interaction exhibits a characteristic pattern of charge concentration and of charge depletion in terms of the Laplacian of ρ, both in an absolute sense and in relation to the positioning of the interatomic surface as determined by ρ and its associated gradient vector field.

It is also possible to observe behavior transitional between shared and closed-shell interactions in the absence of charge transfer. In the homonuclear series $B_2 \rightarrow F_2$ both $\rho(\mathbf{r}_c)$ and $|\nabla^2\rho(\mathbf{r}_c)|$ increase to maximum values at N_2 and decrease again to minimum values at F_2. This behavior parallels the binding energies of these molecules as it does the occupation of the $1\pi_u$ bonding molecular orbital (fully occupied at N_2) and of the $1\pi_g$ antibonding orbital (fully occupied at F_2). As noted above, and as anticipated by molecular orbital theory, an increase in the occupation of the $1\pi_g$ orbital leads to an increase in the localization of charge on each atom and this has the expected consequences on the properties of ρ at $\mathbf{r}_c$; namely, a decrease in $\rho(\mathbf{r}_c)$ and an increase in the positive curvature λ_3. In F_2, the contraction of ρ towards each nucleus dominates the interaction (see Fig. 7) and $\nabla^2\rho > 0$ along almost the entire length of the interaction line. The characteristics of ρ at $\mathbf{r}_c$ for $F_2(\cdots 1\pi_g^4)$ are intermediate between those for $O_2(\cdots 1\pi_g^2)$ and $Ne_2(\cdots 1\pi_g^4 3\sigma_u^2)$ (see Table I); $\rho(\mathbf{r}_c) = 0.296$, $\nabla^2\rho(\mathbf{r}_c) = 0.233$, $\lambda_1 = \lambda_2 = -0.731$, and $\lambda_3 = 1.694$, all in atomic units. The ratio $G(\mathbf{r}_c)/\rho(\mathbf{r}_c) = 0.86$ is less than unity as in O_2. The ratio of the kinetic energy

TABLE III. Characterization of atomic interactions in diatomic hydrides.[a]

AH	R	$\rho(\mathbf{r}_c)$	$\nabla^2\rho(\mathbf{r}_c)$	$\lambda_1=\lambda_2$	λ_3	$\lvert\lambda_1\rvert/\lambda_3$	$G_\perp/G_\parallel$[b]	$G(\mathbf{r}_c)/\rho(\mathbf{r}_c)$	Net charge[c] on A
LiH $^1\Sigma^+$	3.015	0.0407	0.1571	−0.0619	0.2808	0.2204	0.0	1.017	+0.911
BeH $^2\Sigma^+$	2.538	0.0965	0.1638	−0.2032	0.5703	0.3563	0.0	0.950	+0.868
BH $^1\Sigma^+$	2.336	0.1843	−0.5847	−0.4622	0.3397	1.3606	0.0	0.396	+0.754
CH $^2\Pi$	2.124	0.2787	−1.0389	−0.7572	0.4754	1.5928	2.231	0.102	+0.032
NH $^3\Sigma^-$	1.961	0.3395	−1.6034	−1.2399	0.8765	1.4146	2.196	0.157	−0.323
OH $^2\Pi$	1.834	0.3756	−2.6482	−1.8968	1.1454	1.6560	2.527	0.208	−0.585
FH $^1\Sigma^+$	1.733	0.3884	−4.3872	−2.8015	1.2159	2.3041	2.990	0.251	−0.760
NaH $^1\Sigma^+$	3.566	0.0337	0.1320	−0.0394	0.2108	0.1869	0.0426	0.979	+0.810
MgH $^2\Sigma^+$	3.271	0.0529	0.1844	−0.0695	0.3233	0.2150	0.0398	1.023	+0.796
AlH $^1\Sigma^+$	3.114	0.0743	0.1883	−0.1054	0.3990	0.2642	0.0368	0.981	+0.825
SiH $^2\Pi$	2.874	0.1134	0.1330	−0.1666	0.4663	0.3573	0.0763	0.9330	+0.795
PH $^3\Sigma^-$	2.708	0.1590	−0.1142	−0.2222	0.3302	0.6729	0.1961	0.7679	+0.579
SH $^2\Pi$	2.551	0.2128	−0.5663	−0.3732	0.1801	2.0722	1.385	0.2617	+0.094
ClH $^1\Sigma^+$	2.409	0.2540	−0.7824	−0.6035	0.4247	1.4210	2.536	0.2327	−0.241

[a] All quantities in atomic units. The results are calculated from functions using a Slater basis of near Hartree–Fock quality; P. E. Cade and W. M. Huo, At. Data Nucl. Data Tables **12**, 415 (1973).
[b] In a single determinant state function comprised of σ orbitals only $G_\perp(\mathbf{r}_c)=0$.
[c] Determined by the integration of $\rho(\mathbf{r})$ over the basin of the atom (see Ref. 41).

components at

$$\mathbf{r}_c(G_\perp/G_\parallel = 0.751)$$

while less than unity as typical of a closed-shell interaction, is considerably greater than the corresponding value for Ne_2.

The pronounced contraction of ρ towards each atomic centre in F_2 yields atomic charge distributions of a highly localized nature. If the electronic density in F_2 was separately localized within the boundaries of each F atom, a corresponding atomic integration of the Fermi correlation would equal $-\bar{N}(F)$, minus the average population of a F atom.[19] In this limit of complete localization, as is realized only in the separated atoms, there would be no exchange of electrons between the F atoms. What is remarkable is the extent to which this limiting case of atomic localization of the pair and number densities is approached in F_2, its value being 93%. In this molecule the interatomic surface maximizes the extent of intra-atomic Fermi correlation and minimizes the fluctuation in $\bar{N}(F)$. The contribution to the exchange integrals arising from *inter*atomic electron exchange (a measure of covalent binding in the molecular orbital model of electronic structure) is correspondingly small. In contrast, the corresponding extents of atomic localization in C_2 and N_2 are 73% and 78%, respectively. For these two molecules the interatomic surfaces *maximize* the fluctuations in the atomic populations.

Thus the strong potential field exerted on the valence electrons in a fluorine atom while providing the major source of binding in fluorides via a charge transfer to the fluorine atom, is also the cause of the weak binding found in F_2.[19] The

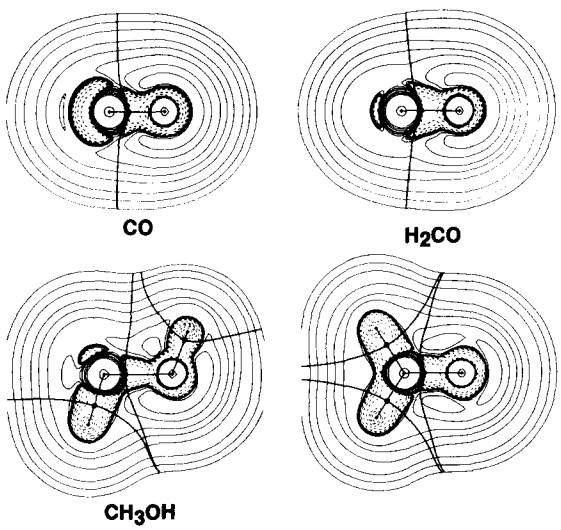

FIG. 6. Contour maps of the Laplacian of ρ for carbon monoxide, the plane containing the framework H–C–O–H of methanol and on the right-hand side, two planes of formaldehyde. Note the difference in the degree and extent of the concentration of charge on the nonbonded side of the C atom in CO and CH_2O by comparing the two top diagrams.

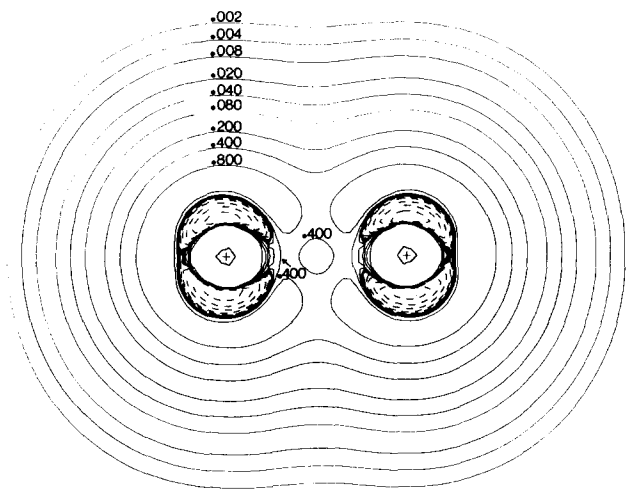

FIG. 7. Contour map of the Laplacian of ρ for the F_2 molecule. The values of the positive contours are given to indicate that the extent of charge depletion is greater in the nonbonded regions than in the internuclear region. The interaction of two *F* atoms is dominated by a contraction of ρ towards each nucleus, to the extent that the usual atomic pattern of a ring-like region of charge increase around each nucleus is disrupted. The innermost negative contour has a value of −8.0 a.u.

atomic interaction in F_2 is qualitatively different from that for the other bound A_2 diatomics. It exhibits characteristics typical of those found for the final member of the series, Ne_2 as a consequence of the very pronounced intra-atomic correlation present in a fluorine atom.

V. INTERACTIONS IN BOUND AND UNBOUND STATES

We now consider the problem of further classifying a given interaction as belonging to a bound or unbound state of a system, i.e., bound or unbound with respect to a separation of the system into the two fragments linked by the corresponding interaction line. This problem is first considered from the electrostatic point of view wherein the regions of charge concentration as determined by the Laplacian of ρ are related to the forces acting on the nuclei.[35] This is followed by a discussion of the energetics of interactions in terms of the regions of dominant potential and kinetic energy contributions to the virial as again determined by the Laplacian distribution of the charge density.

In the fixed nucleus approximation the Hellmann–Feynman theorem applies[36] and the force on a nucleus is determined by the electrostatic field of ρ and that of the other nuclei at the position of the nucleus.[37] A necessary condition for a state to be bound is that it possess at least one configuration of the nuclei for which the electrostatic or Hellmann–Feynman force is zero for each nucleus. If for some interaction the force of the electrons is attractive (tending to decrease R) and this force exceeds in magnitude the nuclear force of repulsion for some finite range of internuclear separations $R \geqslant R_e$ where R_e is the equilibrium separation, then the system is bound, i.e., the energy increases for an increase or decrease in R about $R = R_e$.

The Laplacian distributions for the systems with shared interactions illustrated in Figs. 3–6 are for bound systems in their equilibrium geometries. In all of these molecules $\nabla^2\rho < 0$ over the binding region[37,38] of each interacting pair of nuclei. Thus in shared interactions, electronic charge is concentrated in the internuclear region as a result of the contractions of ρ towards the bond path and this concentration of charge extends over the atomic basins of both nuclei. It is this shared concentration of charge which exerts the net attractive forces on the nuclei for $R > R_e$ and balances the nuclear force of repulsion at R_e. While $\nabla^2\rho < 0$ in the antibinding regions of nuclei in diatomic molecules, the amount of electronic charge concentrated in these regions is less than that accumulated in the binding region and the net force exerted by ρ on the nuclei is one of attraction, equal and opposite to the nuclear force of repulsion at $R = R_e$.

In a shared interaction it is the electronic charge concentrated in the neighborhood of the interatomic surface and extending over both atomic basins which exerts the attractive forces on the nuclei. In the closed-shell interactions this same region in the neighborhood of the interatomic critical point is one of charge depletion and charge is instead concentrated separately in each atomic basin in shell-like regions similar to those found in an isolated atom or ion. Clearly, such an interaction can result in a bound or unbound state depending upon the direction of the polarization of each atomic charge distribution. The directions of these polarizations of the total density are apparent in the Laplacian distributions of ρ. The Laplacian map for Ar_2 shown in Fig. 3 shows that more electronic charge is concentrated on the nonbonded than on the bonded side of each argon atom. The map also indicates that charge is depleted from the region between the nuclei to a greater extent than it is from the nonbonded region of each nucleus. Thus the net forces on the nuclei are repulsive in accordance with the unbound nature of this state. Similar properties are exhibited by the Laplacian maps for other noble gas diatomics for values of R less than the value of R_e for the van der Waal's minimum.

The remaining distributions shown in Fig. 3 for closed-shell interactions are for bound states of ionic systems at their equilibrium geometries. Elementary considerations[34,37] show that for an ionic molecule to achieve electrostatic equilibrium the charge distributions of both the anion and cation must be polarized in a direction counter to the direction of charge transfer. The cationic nucleus is attracted by the net negative field of the anion and the charge distribution of the cation must polarize away from the anion to balance this attractive force. The anionic nucleus is repelled by the net positive field of the cation and the charge distribution of the anion must polarize towards the cation to balance this repulsive force. Such polarizations are evident in the Laplacian maps for the large and more polarizable chloride and potassium ions.[39] A more detailed display of $\nabla^2\rho$ shows that the predicted polarizations are also present in the Laplacian distributions of the less polarizable fluoride and lithium ions. The same observations hold for the LiH and NaH molecules in Fig. 5. In ionic systems the nearly complete transfer of the valency density of one atom to the other yields two closed-shell structures and both nuclei are bound by the net negative electric field exerted by the inwardly polarized charge concentrated within the basin of the anion.[34]

While the Hartree–Fock result for F_2 does not predict a bound state with respect to the energy of two separated fluorine atoms, the Hartree-Fock charge density does predict a value of R for which the Hellmann–Feynman forces on the nuclei vanish. Since this interaction is dominated by the contraction of charge density towards each of the nuclei, the attainment of electrostatic equilibrium must be a result of polarizations of ρ within each atomic distribution. From the Laplacian map for F_2 shown in Fig. 7 it is clear that the charge density is depleted to a greater extent in the antibinding than in the binding region of each fluorine atom and electrostatic equilibrium and a weak bond are obtained almost by default. To the extent that the Hartree-Fock charge density for F_2 is qualitatively correct, the mechanism of binding in F_2 is more analogous to that found in the closed-shell interactions than it is to that of the shared interactions in molecules such as N_2 and O_2. The charge density of a fluorine atom, free or combined, is both tightly bound and strongly localized within the boundary of the atom. These properties, while accounting for the strong binding found for fluoride molecules with significant charge transfer, are the antithesis of those required for the formation of a strong bond in F_2.

The Laplacian maps in Fig. 5 for the diatomic hydrides show that there is a smooth transition in the mechanism of

binding from that of the ionic limit in LiH and NaH to that characteristic of the shared interactions. In the intermediate cases the charge concentrated in the basin of the hydrogen is increasingly polarized towards A and eventually is concentrated over both atomic basins. In these intermediate cases the "back polarization" of the valence charge density on A is much more pronounced than the polarization of the cationic core density in the ionic systems. The core densities of the A atoms in the intermediate cases are in fact slightly polarized towards the proton.[34,35]

A hydrogen bond is another example of a closed-shell interaction which leads to the formation of a bound system. The Laplacian maps for the dimers of HF and H_2O (Fig. 4) show that, as is typical of a closed-shell interaction, the formation of a hydrogen bond does not result in a new region of charge concentration and the form of $\nabla^2\rho$ over each monomer fragment is similar to that for the isolated monomer. In the examples reported here, the transfer of charge between the interacting molecules is minimal and the binding, from the electrostatic point of view (i.e., in terms of the forces exerted on the nuclei), is primarily a result of a change in the polarizations present in each of the monomers. The directions of the polarization changes mimic the polarizations found in the closed-shell ionic molecules with the acid, the proton donor, behaving as the cation and the base as the anion.

Only the structurally simple HF dimer is considered in detail. The dimer of H_2O yields identical observations. Figure 8 summarizes the net charges on each atom in the monomer, the magnitudes and directions of the atomic dipoles in the monomer and the *change in these quantities* in forming the dimer.[40] The atomic populations and dipoles are obtained by an integration of ρ and $\mathbf{r}\rho$, respectively, over the basin of each atom.[41] The transfer of charge in HF is considerable and each atomic density is polarized in a direction counter to the direction of this transfer. There is a small enhancement in the extent of charge transfer accompanied by reductions in the atomic polarizations, in both fragments of the dimer and the dipole moment ($\overrightarrow{HF}$) of each fragment is thereby increased. The largest reduction in charge, of 0.026 e^-, occurs for the hydrogen bonded proton.[42] The atomic dipole of the F of the base fragment has a component in the direction of this proton. Thus relative to an isolated monomer, the charge distribution of the base fragment is polarized in the direction of the acid fragment, which in turn is polarized away from the base. These polarizations are greatest for the negatively charged F of the base and the positively charged *H* of the acid and the mechanism of achieving electrostatic equilibrium is the same as that found in the closed-shell ionic interactions. The polarizations of the F and O atoms of the base fragments towards the proton of the proton donor are evident in the $\nabla^2\rho$ maps (Fig. 4).

A single determinant SCF calculation using a 6-21G* basis predicts a weakly bound and linear geometry for the van der Waals molecule ArHCl. While such a calculation is admittedly insufficient with regards to its neglect of electron correlation in such an interaction, the charge density at the critical point of the Ar–H interaction exhibits the properties characteristic of a closed-shell interaction: a low value for

$$\rho(\mathbf{r}_c) = 1.8\times10^{-3}\ \text{a.u.}$$

$$\nabla^2\rho(\mathbf{r}_c) = +6.2\times10^{-3}\ \text{a.u.}$$

and $|\lambda_1|/\lambda_3 = 0.15$. The binding in this molecule is understandable in terms of the properties characteristic of a bound polarized closed-shell interaction as found in a hydrogen bonded system: (a) the charge density of the Ar is polarized towards the *H*; (b) a small increase in the extent of charge transfer from H to Cl and a reduction in the counter polarizations of the H and Cl atoms present in an isolated HCl molecule; (c) no significant charge transfer between Ar and HCl. As predicted by Feynman[36] and substantiated by studies of a charge distribution obtained from a correlated state function[43,44] the van der Waals attractive force between two neutral spherical atoms observed for large internuclear separations results from a polarization of each atomic distribution in the direction of the approaching atom. Thus a closed-shell interaction between two neutral atoms is attractive for values of *R* at which no significant overlap between the atomic densities occurs. The major effect of electron correlation on the Ar in ArHCl could be a similar polarization of its charge density, enhancing the atomic dipole induced by the proximity of HCl.

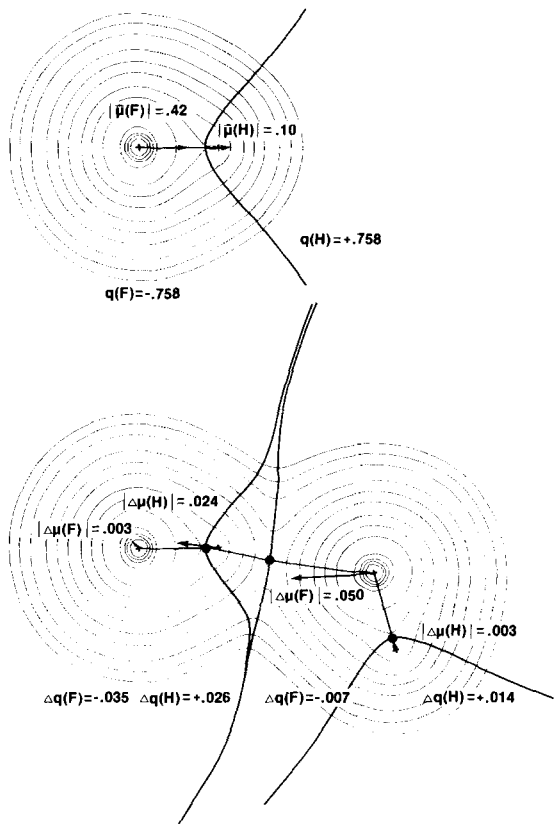

FIG. 8. Contour maps of the charge distributions of HF monomer and dimer. (Contour values are those given for Fig. 1.) The values of the atomic net charges *q* and of the atomic dipoles $|\mu|$ are given for the monomer. The *changes* in these values in forming the dimer and the directions of the changes in the atomic dipoles are given for the dimer. Note that in the monomer the contour of value 0.40 encompasses the proton while in the dimer this contour encircles only the F nucleus. There is a transfer of electronic charge from H to F in both fragments of the dimer. (The values of ρ at the proton in the monomer and in the acid and base of the dimer are, respectively, 0.416, 0.393, 0.398 a.u.)

A. Mechanics of atomic interactions

The Laplacian of ρ determines the regions of space where electronic charge is concentrated. This function, coupled with the Hellmann–Feynman theorem enables one to qualitatively characterize a charge distribution as binding or antibinding with respect to a given interaction in a molecule. These same regions of space, those where $\nabla^2\rho < 0$, are the regions in which the potential energy makes dominant contributions to the virial of a system. Thus the Laplacian of ρ provides a link between the forces acting on the nuclei and the energetics of an interaction, a link which we now pursue.

In the fixed nucleus approximation the virial of the (Ehrenfest) forces exerted on the electrons in a molecule, the electronic potential energy, is

$$-\int \mathbf{r}\cdot\nabla\cdot\ddot{\sigma}(\mathbf{r})d\mathbf{r} = \mathscr{V} = V_{ne} + V_{ee} - \sum_\alpha \mathbf{X}_\alpha \cdot \int \nabla\hat{v}_\alpha \rho(\mathbf{r})d\mathbf{r}, \tag{25}$$

where $\mathbf{X}_\alpha$ is a nuclear position coordinate and $\hat{v}_\alpha$ is the electron–nuclear potential energy operator. The terms on the right-hand side of Eq. (25) are, respectively, the electron–nuclear and electron–electron potential energies and virial of the Hellmann–Feynman forces exerted on the electrons by the nuclei. The latter term may be expressed as

$$-\sum_\alpha \mathbf{X}_\alpha \cdot \int \nabla\hat{v}_\alpha \rho \, d\mathbf{r} = \sum_\alpha \mathbf{X}_\alpha \cdot \int \nabla_\alpha v_\alpha \rho \, d\mathbf{r}$$

$$= V_{nn} + \sum_\alpha \mathbf{X}_\alpha \cdot \nabla_\alpha E, \tag{26}$$

where V_{nn} is the nuclear–nuclear potential energy and the sum is minus the virial of the *net* forces acting on the nuclei. The quantity E, the *total* energy of the molecule, is the sum of the electronic and nuclear energies E_e and E_n, where[45]

$$E_e = T + \mathscr{V}, \tag{27}$$

$$E_n = -\sum_\alpha \mathbf{X}_\alpha \cdot \nabla_\alpha E.$$

Since the nuclei are stationary, E_n is purely potential and equal to the virial of the forces acting on the nuclei. Thus $E = T + V$ where the *total* potential energy V is

$$V = V_{en} + V_{ee} + V_{nn} = \mathscr{V} - \sum_\alpha \mathbf{X}_\alpha \cdot \nabla_\alpha E. \tag{28}$$

The virial theorem may be stated in terms of the electronic contributions to E as

$$T = -E_e = -\tfrac{1}{2}\mathscr{V} \tag{29}$$

or in terms of the total energies as

$$T = -E - \sum_\alpha \mathbf{X}_\alpha \cdot \nabla_\alpha E$$

$$= -\tfrac{1}{2}\left(V + \sum_\alpha \mathbf{X}_\alpha \cdot \nabla_\alpha E\right). \tag{30}$$

For an isolated atom, or for a molecule in an equilibrium configuration one has $T = -E_e = -E$. In general however, for a molecule

$$T = -E_e \gtrless -E \tag{31}$$

depending on whether there are repulsive ($T > |E|$) or attractive ($T < |E|$) forces acting on the nuclei. Thus the vanishing of the integral of the Laplacian density over all space ensures the satisfaction of the virial theorem with respect to the electronic energies, Eqs. (9) and (29), but not necessarily with respect to the total energy.

The Laplacian of ρ via Eq. (16), compares $2G(r)$ not with contributions to the potential energy V, but to $\mathscr{V}$ the electronic potential energy. This is an important distinction from the point of view of whether or not a system is bound. Consider an interaction where $\nabla^2\rho$ is predominantly negative over the binding region and *net* forces of attraction act on the nuclei. In this case the local contribution to the virial of the Hellmann–Feynman forces exerted on the electrons Eq. (26), integrates to a value greater than V_{nn}. Thus because of the concentration of charge in the binding region the *total* potential energy V is more negative than $\mathscr{V}$ [Eq. (28)] $|V| > 2T$ and $|E| > T$. Thus, E decreases with a decrease in R, until V_{nn} increases to a value such that equilibrium is attained and $V = \mathscr{V}$. It is however, the concentration of negative charge in the binding region resulting from contractions in ρ perpendicular to the bond path which causes the local contributions to V to exceed the contributions from the kinetic energy for $R > R_e$ thereby leading to the creation of attractive forces and hence to a shared chemical bond. In a system where $\nabla^2\rho$ is predominantly positive over a binding region and *net* forces of repulsion act on the nuclei, the kinetic energy contributions to the virial dominate over the internuclear region as a result of the contraction of the electronic charge density towards the nuclei and its consequent depletion in this region. In this situation $\nabla^2\rho$ is most negative in the antibinding regions, V is less negative than $\mathscr{V}$, $2T > |V|$ and the system is unbound. In an ionic bond the transfer of charge to the anion for $R > R_e$, and the polarization of its shell-like concentration of charge towards the cation yields net attractive contributions to $\mathscr{V}$ Eq. (25), V exceeds $\mathscr{V}$ in magnitude Eq. (28) and $2T < |V|$.

A comparison of the Laplacian distribution for a shared interaction with its shell-like structure in the separated atoms shows that the major change in this function on the formation of such an interaction is the creation of a region over which $\nabla^2\rho < 0$ extending over the basins of both atoms. This concentration of charge results from a contraction of ρ perpendicular to the interaction line and it leads to a local lowering of the potential energy. The magnitude of this lowering in the potential energy is greater than the contributions to the kinetic energy from the same region, where $\nabla^2\rho < 0$. In particular, the component of the kinetic energy parallel to the bond path is decreased in value as a result of the decreases in the corresponding gradients and curvatures of ρ.

The differing properties of the charge distributions for bound and unbound states are made very clear by comparing the Laplacian distributions of ρ for H_2 and He_2 (Fig. 3). In the former, the atomic interaction is dominated by the contractions in ρ perpendicular to the bond path while in the later it is dominated by the contractions in ρ towards each of the nuclei.

The binding of the nuclei in ring or cage structures is made particularly clear by the Laplacian distribution of the charge density. In cyclopropane the magnitudes of the two negative curvatures of ρ at a carbon–carbon bond critical

point are unequal (Table II). The principal axis of the curvature of smallest magnitude is directed at the ring or (3, + 1) critical point at the center of the ring surface. Thus, a carbon–carbon bond of cyclopropane has a noticeable ellipticity ($\epsilon = 0.490$) and electronic charge is preferentially concentrated in the ring surface[25,46] (Fig. 4). The Laplacian of ρ shows a concentration of valence charge density over the surface of the ring with the exception of a small region in the neighborhood of the (3, + 1) critical point. (The principal axes of the two positive curvatures of a ring critical point lie in and define the ring surface.) It is this concentration of electronic charge in the interior of the ring structure which binds the ring nuclei. The large extent of this concentration of charge is reflected in a noticeable curvature of the bond paths away from the geometrical perimeter of the ring (Fig. 4).

Electron deficient molecules such as the boranes form ring and cage structures to gain maximum stability from a minimum amount of electronic glue by a very pronounced delocalization of charge over ring surfaces. The molecular graph for $B_6H_6^{-2}$ shows each boron atom to be linked to one hydrogen atom and four other boron atoms to form an octahedral cage structure bounded by eight ring surfaces. The Laplacian of the charge density for one such three-membered boron ring surface is shown in Fig. 9. The boron–boron bonds exhibit extreme ellipticities equal to 3.58 and, as illustrated in Fig. 9, electronic charge is concentrated over the whole of the ring surface. The contraction of ρ along the axis perpendicular to the ring surface at the ring critical point is also large and it dominates the two positive curvatures of ρ in the ring surface so that $\nabla^2\rho$ is negative even at the ring critical point. The value of ρ at a ring critical point is 0.120 a.u., only slightly less than its value of 0.127 a.u. at a boron–boron bond critical point. The same observations hold true for four-membered rings involving one or two bridging hydrogen atoms in molecules such as B_2H_6 or B_5H_9. Figure 9 illustrates the Laplacian of ρ in the plane of the bridging hydrogen nuclei of B_2H_6. In this four-membered ring the bond paths are inwardly curved and electronic charge is again delocalized over the valence region of the ring surface. The ellipticities of the B–H bridging bonds equal 0.561 and their values of $\rho(\mathbf{r}_c) = 0.119$ a.u. exceed the value of ρ at the ring critical point by only 0.013 a.u. Thus in three- and four-membered rings of electron deficient structures, electronic charge is preferentially delocalized over and concentrated in the ring surface where it serves to bind all nuclei of the ring. The description of such molecules as globally delocalized[47] is particularly apt.

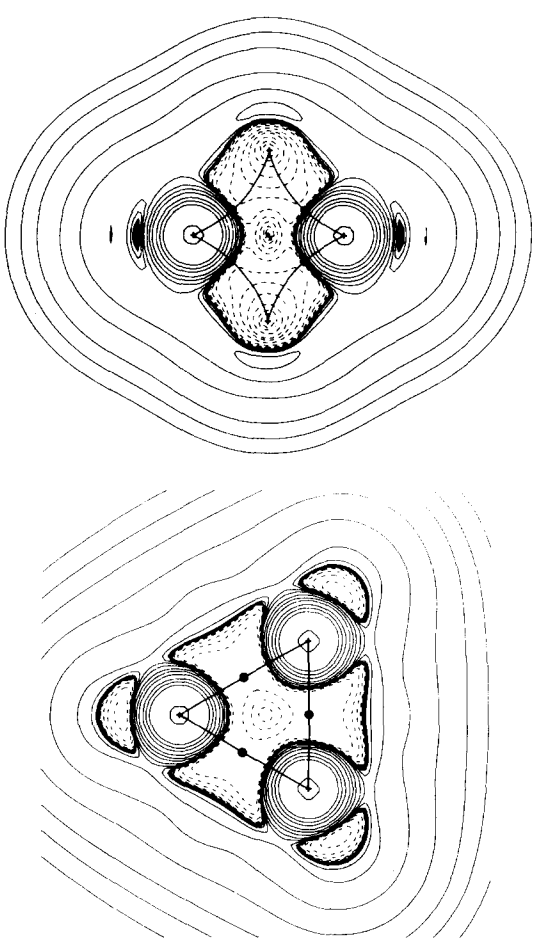

FIG. 9. Contour maps of the Laplacian of ρ for the bridging plane (B–H–B–H) of B_2H_6 and for a plane containing three boron nuclei in the octahedral molecule $B_6H_6^{-2}$.

VI. CONCLUSIONS

Slater regarded the Hellmann–Feynman and virial theorems as "two of the most powerful theorems applicable to molecules and solids."[48] Their use in conjunction with the properties of molecular charge distributions as characterized within the topological theory of molecular structure yields a classification and understanding of atomic interactions. Given a charge distribution, one may define its set of atomic interactions in terms of the gradient vector field of the charge density. The mechanics of the interactions, whether they are bound or unbound and their energetics, as viewed through the virial theorem, are qualitatively understood in terms of the properties of the Laplacian of the charge density. The central problems now focus on the distribution of charge itself. What determines its form? Certain forces must be dominant to yield a form that is so readily mapped onto the chemical concepts underlying the notion of molecular structure.[49] Can the local mechanics of a molecular system, now expressible in terms of the first-order density matrix, be further reduced to equations involving only the charge density? These questions fall in the realm of density functional theory. It is to be hoped that studies such as the present one, which relate properties of ρ to its local mechanics, will aid in the development of density functional models. A model which included, perhaps in the form of a necessary constraint, the nodal properties of the Laplacian distribution of ρ e.g., would most likely recover the structure of the radial distribution function for a many-electron atom.[50] Are there quantitative relations underlying the correlations noted here between the curvatures of ρ and the corresponding components of the kinetic energy density? Further studies from this laboratory will determine whether a structural homeomorphism exists between $\rho(\mathbf{r})$ and the kinetic energy density $G(\mathbf{r})$. The vector field $\nabla\cdot\vec{\sigma}(\mathbf{r})$ which determines the force acting on an element of charge is presently under investigation. Its

topological structure is considerably more complex than that of the *gradient* vector field of the charge density, a result which is perhaps not surprising as it contains considerably more physical information.

[1]R. F. W. Bader and G. R. Runtz, Mol. Phys. **30**, 117 (1975); G. R. Runtz, R. F. W. Bader and R. R. Messer, Can. J. Chem. **55**, 3040 (1977).

[2]K. Collard and G. G. Hall, Int. J. Quantum Chem. **12**, 623 (1977).

[3]R. F. W. Bader, T. T. Nguyen-Dang, and Y. Tal, J. Chem. Phys. **70**, 4316 (1979).

[4]J. Palis and S. Smale, Pure Math. **14**, 223 (1970); R. Thom, *Structural Stability and Morphogenesis* (Benjamin, Reading, Mass., 1975).

[5]R. F. W. Bader, T. T. Nguyen-Dang, and Y. Tal, Rep. Prog. Phys. **44**, 893 (1981).

[6]T. T. Nguyen-Dang and R. F. W. Bader, Physica **114**, 68 (1982).

[7]P. M. Morse and H. Feshbach, *Methods of Theoretical Physics* (McGraw-Hill, New York, 1953), part I.

[8]R. F. W. Bader, J. Chem. Phys. **73**, 2871 (1980).

[9]R. F. W. Bader and T. T. Nguyen-Dang, Adv. Quantum Chem. **14**, 63 (1981).

[10]W. Pauli, *General Principles of Quantum Mechanics* (Springer, Berlin, 1980).

[11]V. H. Smith, J. F. Price, and I. Absar, Israel J. Chem. **16**, 187 (1977).

[12]The molecular structure associated with a given nuclear configuration **X** is stable if $\rho(\mathbf{r},\mathbf{X})$ has a finite number of critical points and (a) each critical point is nondegenerate (of rank three); (b) the stable and unstable manifolds of any pair of critical points intersect transversely (Refs. 4–6).

[13]An atomic property A is determined by an integration of the corresponding density $\rho_A(\mathbf{r})$ over the basin of the atom. The symbol $\int d\tau'$ implies a summation over all spins and an integration over the spatial coordinates of all electrons but one whose coordinates are denoted by **r**. Thus $\langle[\hat{H},\hat{A}]\rangle_\Omega = N\int_\Omega d\mathbf{r}\int d\tau'\psi^*[\hat{H},\hat{A}]\psi$. The quantity **J** is the single-particle vector current density.

[14]K. C. Janda, J. M. Steed, S. E. Novick, and W. Klemperer, J. Chem. Phys. **67**, 5162 (1977).

[15]P. Ehrenfest, Z. Phys. **45**, 455 (1927).

[16]S. T. Epstein, J. Chem. Phys. **63**, 3573 (1975).

[17]R. F. W. Bader and H. Essen, *Local Density Approximations in Quantum and Solid State Physics*, edited by J. P. Dahl and J. Avery (Plenum, New York, 1984).

[18]The Tr $\sigma(\mathbf{r})$ may be expressed as $\{-2G(\mathbf{r}) + (\hbar^2/4m)\nabla^2\rho(\mathbf{r})\}$. Even at, and in the neighborhood of a (3, +3) or cage critical point where all three curvatures of $\rho(\mathbf{r})$ are positive, Tr $\overleftrightarrow{\sigma}(\mathbf{r}) < 0$.

[19]An atomic core region may be defined in terms of an extremum principle as a spherical region of space centered on the nucleus bounded by a surface such that the contained Fermi correlation is maximized. This corresponds to finding, a region for which the fluctuation in the average electron population is a minimum and in which the electron number and pair densities are maximally localized. [R. F. W. Bader and M. E. Stephens, J. Am. Chem. Soc. **97**, 7391 (1975).] Such core regions in general exist and are *found* to possess an average population $\bar{N}$ of approximately two electrons. Some values of $\bar{N}$, radius r and % localization are 2.0, 0.53 a.u. and 88% for C; 2.0, 0.26 a.u. and 77% for Ne; 1.9, 0.12 a.u. and 73% for the K shell in Ar and 10.1, 0.75 a.u. and 80% for its combined K and L shells. It has also been proposed that the first minimum in the radial distribution function for an atom be used to define a core radius [P. Politzer and R. G. Parr, J. Chem. Phys. **64**, 4634 (1976)]. In general, these radii are slightly greater than those defined by minimizing the fluctuation in $\bar{N}$ as described above.

[20]The relationship in Eq. (17) is found to be only approximately true for many-electron atoms using Hartree–Fock state functions in the calculations. In these systems the constant of proportionality equal to 0.541 in Eq. (17) exhibits a small Z dependence and its value decreases from 0.534 for He to 0.424 for Ne.

[21]In a one-electron atom the curvature of ρ parallel to a radial line λ_3, is always positive. In a many-electron atom λ_3 may become slightly negative over a very short range of radial distances r, near the inner boundary of the valence region, where $\nabla^2\rho < 0$. For example, in Ar, $\lambda_3 < 0$ for $1.01 \leqslant r \leqslant 1.23$ a.u. In this situation the magnitude of λ_3 is less than the magnitudes of the perpendicular curvatures of ρ.

[22]R. F. W. Bader and P. M. Beddall, J. Chem. Phys. **56**, 3320 (1972).

[23]Deb and Bamzai [B. M. Deb and A. S. Bamzai, Mol. Phys. **35**, 1349 (1978); **38**, 2069 (1979)] have constructed a stress tensor in terms of the electronic *and* nuclear charge distributions applicable to one-electron and singlet ground states of a two-electron system within a single determinant approximation, i.e., $\mathbf{F}(\mathbf{r})$ is conservative. They have studied the properties of this tensor in the hydrogen atom and have used it in a discussion of the binding in the H_2 molecule.

[24]In a bound system, an atomic interaction line is called a bond path.

[25]R. F. W. Bader, T. S. Slee, D. Cremer, and E. Kraka, J. Am. Chem. Soc. **105**, 5061 (1983). D. Cremer, E. Kraka, T. S. Slee, R. F. W. Bader, T. T. Nguyen-Dang, and P. MacDougall, J. Am. Chem. Soc. **105**, 5069 (1983).

[26]R. F. W. Bader and H. J. T. Preston, Int. J. Quantum Chem. **3**, 327 (1969).

[27]Displays of the kinetic energy density $G(\mathbf{r})$ for H_2 and He_2 are given in Ref. 26. To appreciate the dramatically low values attained by $G(\mathbf{r})$ and in particular its parallel component in H_2, the reader is referred to Fig. 1 of this reference for a profile of $G(\mathbf{r})$ along the internuclear axis calculated using a correlated state function.

[28]C. A. Coulson, Proc. Cambridge Philos. Soc. **37**, 55, 74 (1941); C. A. Coulson and W. E. Duncanson, *ibid.* **37**, 67, 406 (1941).

[29]I. R. Epstein and A. C. Tanner, in *Compton Scattering*, edited by B. Williams (McGraw-Hill, New York, 1977), pp. 216–232.

[30]B. I. Ramirez, Chem. Phys. Lett. **94**, 180 (1983).

[31]W. H. Henneker and P. E. Cade, Chem. Phys. Lett. **2**, 575 (1968).

[32]W. Weyrich, *Einige Beiträge Zur Compton-Spektroskopie*, Habilitationsschrift Technische Hochschule Darmstadt, Darmstadt, June, 1978.

[33]P. Pattison and W. Weyrich, J. Phys. Chem. Solids **40**, 213 (1979).

[34]The properties of the total charge distributions for A_2, AH, and AB molecules have been given previously: for A_2, R. F. W. Bader, W. H. Henneker and P. E. Cade, J. Chem. Phys. **46**, 3341 (1967); B. J. Ransil and J. J. Sinai, *ibid.* **46**, 4050 (1967); R. F. W. Bader and A. K. Chandra, Can. J. Chem. **46**, 953 (1968); for AH, R. F. W. Bader, I. Keaveny, and P. E. Cade, J. Chem. Phys. **47**, 3381 (1967); P. E. Cade, R. F. W. Bader, W. H. Henneker, and I. Keaveny, *ibid.* **50**, 5313 (1969); R. F. W. Bader and P. M. Beddall, J. Am. Chem. Soc. **95**, 305 (1973); R. F. W. Bader and R. R. Messer, Can. J. Chem. **52**, 2268 (1974): for AB, R. F. W. Bader and A. D. Bandrauk, J. Chem. Phys. **49**, 1653 (1968); R. F. W. Bader and W. H. Henneker, J. Am. Chem. Soc. **87**, 3063 (1965); **88**, 280 (1966).

[35]Previous studies (Ref. 34) of the binding or antibinding nature of a molecular charge distribution have made use of density difference maps wherein superposed atomic densities are subtracted from the molecular density. Such studies suffer from a degree of arbitrariness in the choice of the atomic reference state and in the nonrealizable nature of the superposed atomic density distribution. The Laplacian distribution of ρ determines the regions of charge depletion and charge concentration without recourse to a reference state.

[36]R. P. Feynman, Phys. Rev. **56**, 340 (1939).

[37]R. F. W. Bader, *The Force Concept in Chemistry*, edited by B. M. Deb (Van Nostrand-Reinhold, New York, 1981), p. 39.

[38]T. Berlin, J. Chem. Phys. **19**, 208 (1951).

[39]The relative positionings and magnitudes of the regions where $\nabla^2\rho \lesssim$ for K in KF (Fig. 3) show it to be back polarized. One notes that the pattern of $\nabla^2\rho$ for K in KF including its polarization, are similar to those for an argon atom in Ar_2 as anticipated on the basis of the orbital shell model and the ionic model for KF.

[40]These results are calculated from a single determinant SCF function using a 6-31G** Gaussian basis at the optimized geometry. The geometries and binding energies compare favorably with previous calculations. For example, Tse *et al.* [Y.-C. Tse, M. D. Newton, and L. C. Allen, Chem. Phys. Lett. **75**, 350 (1980)] in a 6-31G* calculation of $(H_2O)_2$ calculate a hydrogen bond energy of 5.64 kcal/mol, an O–O separation of 2.98 Å and a value of 55° for the angle θ between the O–O vector and the plane of the proton acceptor. The corresponding values obtained in the present research are 5.50 kcal/mol, 2.99 Å and $\theta = 54°$. The total energy of $(H_2O)_2$ is found to be $-152.056\,00$ a.u. The energy of $(HF)_2$ at 6-31G** is $-200.031\,98$ a.u., yielding a hydrogen bond energy of 5.88 kcal/mol, an F–F separation of 2.68 Å and an H–F...H angle of 115.5°. The F...H–F angle is calculated to be 170.4°. The calculated results compare favorably with experimental results (see, P. A. Kollman, *Electronic Structure Theory*, edited by H. F. Schaefer III (Plenum, New York, 1977), pp. 109–152): $(H_2O)_2$, hydrogen bond energy is 5.2 ± 1.5 kcal/mol and O–O separation is 2.98 Å; $(HF)_2$, hydrogen bond energy is 7.0 ± 1.5 kcal/mol and F–F separation is 2.80 Å.

[41]F. W. Biegler-König, R. F. W. Bader, and T.-H.Tang, J. Comput. Chem. **13**, 317 (1982); F. W. Biegler-König, T. T. Nguyen-Dang, Y. Tal, R. F. W. Bader, and A. J. Duke, J. Phys. B **14**, 2739 (1981).

[42]Tse, Newton and Allen (Ref. 40) find the population of the hydrogen to decrease on hydrogen bond formation when the populations are determined using Mulliken's method.

[43]R. F. W. Bader and A. K. Chandra, Can. J. Chem. **46**, 953 (1968).

[44]J. O. Hirschfelder and M. A. Eliason, J. Chem. Phys. **47**, 1164 (1967).
[45]These definitions of E_e, E_n, and E follow directly from the identification of the virial of the forces acting on a set of particles with their potential energy [S. Srebrenik and R. F. W. Bader, J. Chem. Phys. **63**, 3945 (1975)] as is done in classical mechanics when the forces are conservative. Indeed, for a system with nonconservative forces the variation of the classical action integral $\int(T-V)dt$ is replaced by a variation of the integral

$$I=\int\left(T+\sum_i \mathbf{r}_i\cdot\mathbf{F}_i\right)dt,$$

i.e., if V is undefined it is replaced by the virial of the forces acting on the particles. The variation of the integral I is also employed for the description of a system acted on by forces of constraint. This is the particular case of interest in quantum chemistry, for solving $H\psi=E\Psi$ in the fixed nucleus approximation is such a problem—external forces act on the nuclei to hold them in the fixed geometry. Thus the electronic energy E_e may be obtained by extremizing the variation of the electronic kinetic energy and the virtual work of the electrons. The Hamiltonian which yields the average energy E_e is

$$\sum_i\left(-\frac{1}{2}\nabla_i^2-\mathbf{r}_i\cdot\nabla_i\hat{V}\right),$$

a sum of a kinetic energy operator and an effective single-particle potential energy operator for each electron in the system. This is a *constrained* variation in which the virtual work of the forces of constraint (the external forces acting on the nuclei) must vanish. [S. Srebrenik, R. F. W. Bader and T. T. Nguyen-Dang, J. Chem. Phys. **68**, 3667 (1978), and reference 9].
[46]The in-plane 'π-like' nature of the CC bonds in cyclopropane is accounted for in molecular orbital theory through the choice of a particular orbital representation, the so-called Walsh orbitals. [A. D. Walsh, Nature **159**, 712 (1947); Trans. Faraday Soc. **45**, 179 (1949).]
[47]R. B. King and D. H. Rouvray, J. Am. Chem. Soc. **99**, 7834 (1977).
[48]J. C. Slater, J. Chem. Phys. **57**, 2389 (1972).
[49]Y. Tal and R. F. W. Bader, Phys. Rev. A **21**, 1 (1980).
[50]Wen-Ping Wang and R. G. Parr, Phys. Rev. A **16**, 891 (1977).